Lanthanide-labeled DNA

Paul R. Selvin
Physics Dept. and Biophysics Center
University of Illinois
Urbana, IL 61801

Selvin@uiuc.edu
(217) 244-3371 (tel)
(217) 244-7187 (fax)

Submitted as a chapter in
"Topics in Fluorescence Spectroscopy"
Vol. 7
Ed. Joe Lakowicz

Overview

Lanthanide ions can have highly unusual emission characteristics in aqueous solution, including long (millisecond) excited-state lifetimes, sharply spiked emission spectra (< 10 nm width), and large Stokes shift (> 150 nm). These characteristics, when using pulsed excitation in combination with time-delayed and wavelength-filtered detection, are advantageous for discriminating against background fluorescence, which tends to be short lived (primarily nanosecond) and broadly spread in wavelength. For this reason, lanthanide ions are of significant interest as alternatives to conventional fluorophores, particularly when autofluorescence is a problem. This is particularly true in high-throughput screening assays for drug development where autofluorescence commonly limits sensitivity with conventional probes and radioactivity has undesirable environmental, health, and cost considerations. Detection sensitivity of 10^{-12} – 10^{-15} M can be achieved with lanthanides, exceeding sensitivity achievable with conventional fluorophores and approaching or equaling radioactivity. A number of companies have commercially available lanthanide-based assays although availability of the chelates remains an issue for many university researchers.

A second area of practical and fundamental interest is the use of lanthanide ions as donors in resonance energy transfer studies for the detection of binding between biomolecules or the measurement of nanometer-scale distances within and between biomolecules. It has recently been realized that lanthanide ions make excellent donors in energy transfer experiments, enabling distances up to 100 Å feasible with greatly improved accuracy compared to conventional fluorescent probes. Lanthanide-based resonance energy transfer (LRET) has been applied in both basic and applied studies, including DNA and DNA-protein complexes. Very recently, it has been realized that LRET can lead to new classes of DNA-dyes with tunable excited-state lifetimes in the 10-500 μsec time regime and tunable color emission, from 500 nm to >700nm, which may lead to many advantages, including greatly multiplexed detection of simultaneous signals.

A number of reviews have been written on the use of lanthanide probes, typically in time-resolved measurements, including their use in DNA assays (8, 25-28, 56, 71, 75, 76, 85). This chapter focussed on lanthanides applied to DNA but examples of lanthanides used in protein studies are included because the logical extension to DNA studies is clear in many cases, and indirect detection of DNA through the use of proteins (such as streptavidin) is common. Lanthanide chelates as detection reagents are first discussed, followed by their use in resonance energy transfer studies.

Lanthanides as luminescent labels.

Many of the lanthanide atoms, also known as rare-earth atoms, are widely used as luminescent materials. For example, Neodymium is used in lasers; erbium is used in telecommunication devices; terbium, europium and occasionally gadolinium are used in

fluorescent bulbs. However, in aqueous systems, only europium and terbium have significant luminescence, with dysprosium and samarium being used rarely, and the others not at all. Europium emits primarily in the red, and terbium primarily in the green. Even with europium and terbium, to get significant luminescence in aqueous solution two steps must be taken. First, water must be prevented from binding the lanthanide since water highly quenches its excited-state. This is generally accomplished by encapsulating the lanthanide in a chelate which binds the lanthanide tightly and expels water. In addition, the chelate often serves as a means for attachment of the lanthanide to a biomolecule via some thiol- or amine- reactive functionality. Second, because the lanthanide absorption cross-section is extremely weak (typically $< 1\ M^{-1}cm^{-1}$, compared to $\approx$ 100,000 $M^{-1}cm^{-1}$ for many conventional fluorophores), an antenna (or "sensitizer") is placed near the lanthanide, usually via covalent attachment of the antenna to the chelate. This antenna, usually an organic chromophore, absorbs the excitation light and transfers the energy to the lanthanide, which then re-emits characteristic lanthanide luminescence (94).

Representative Chelates. Figure 1 shows a number of luminescent lanthanide complexes, most of which have been attached to amino-modified nucleotides and others which have been made as phosphoramidites (48, 70). Luminescent cryptates were originally developed by Lehn et al. where the bipyridine antenna molecules are an integral part of the chelation complex (53). Both Eu and Tb are luminescent although they are primarily used with Eu because Tb has a back transfer of energy to the antenna molecule which leads to lanthanide quenching (1). They are used in commercial assays by Cis-Biointernational (Cedex, France) (61-63, 66) and Packard (Meriden, CT, USA). The chelate and sensitizers are also an integral unit in the terpyridine complex developed by Saha et al., which is luminescent with Eu (69), and in the BCPDA complex (4,7-bis(chlorosulfophenyl)-1,10-phenanthroline-2,9-dicarboxylic acid) developed by Diamandis et al. and originally marketed by CyberFluor (Toronto, Canada).

Polyaminocarboxylate chelates, such as diethylenetriaminepentaacetic acid (DTPA), covalently attached to a number of possible antenna molecules, have been widely used, primarily because of their ease of synthesis, good chelation properties, and the ability to independently tailor the chelate and sensitizer for the desired properties (3, 11, 54). Paraaminosalicylate was the original antenna used (3) with DTPA and is luminescent with terbium but not europium. It is hydrophilic, which is advantageous when attaching many chelate-complexes to a biomolecule (see below, *multiple labeling*) but requires fairly short wavelength excitation ($\leq$ 308 nm) with limited brightness. The antenna molecule carbostyril 124 (54) or its derivatives (15), used with polyaminocarboxylate chelates, are brighter and can be excited at 340 nm or longer but are more hydrophobic (54). They have also been shown to be excellent donors in resonance energy transfer applications (discussed below). Savitsky attached up to four β-diketone antenna molecules to a DTPA (72). This system required the use of excess Eu and the presence of detergent and trioctylphosphinoxide but claimed sensitivity equal to the DELFIA system (see below), which is generally the most sensitive lanthanide-based system. In general it is difficult to compare the brightness of various chelates because a side-by-side comparison has not been

published, although some listing of sensitivities have been summarized (28) and are presented below.

An alternative methodology is to use a non-luminescent lanthanide chelate as a label, instead of the luminescent labels discussed above (Fig. 3). After specifically binding the label to the biomolecule of interest, the lanthanide is extracted from the chelate, usually by dropping the pH, and placed in an "enhancement solution" where the lanthanide is luminescent. The enhancement solution typically contains a chelate in a micellar environment (to eliminate quenching effect of water) with organic chromophores (to act as antenna molecules). The commercially available DELFIA (dissociation-enhanced lanthanide fluorescence immunoassay) from Wallac Inc. utilizes this method and is based on $Eu(NTA)_3(TOPO)_2$, (europium-naphthoyltrifluoroacetone-triocylphosphine oxide) in the presence of the non-ionic detergent Triton-X. Tb can also be used at reduced sensitivity compared to Eu, and Dy and Sm can be used with yet a further reduction in sensitivity. One clear disadvantage of the system is that all spatial information is lost, precluding applications such as fluorescence in situ hybridization (FISH). A second disadvantage is the extra steps are required. An advantage of the system, however, is that the detection sensitivity is typically an order of magnitude or more better than directly luminescent chelates.

Fig. 2 shows a representative emission spectra and lifetime for Tb^{3+} and Eu^{3+}. The relative intensities in each peak, particularly with Eu, are a function of chelate structure (symmetry), and the excited-state lifetimes also vary by chelate. All complexes require UV excitation, ranging from 280 nm to approximately 365 nm (see (38) for a discussion of the photophysics). The transitions from excited- to ground state are spin and parity forbidden and hence long-lived. Formally these transitions are not called phosphorescence because they do not arise from a triplet to singlet state (8). Importantly, lanthanide lifetimes in many chelates are not sensitive to oxygen concentration, in contrast to phosphorescent probes. The quantum yield for emission at room temperature is reported to be as high as 0.7, orders of magnitude higher than phosphorescent probes (38, 97). Emission is also highly spiked in wavelength, enabling color-discrimination against background signals. Their spiked spectra is also important when using lanthanides as donors in resonance energy applications because it enables the donor emission to be separated from acceptor emission (see below).

Fig. 1. Some luminescent lanthanide chelate complexes. See text for details.

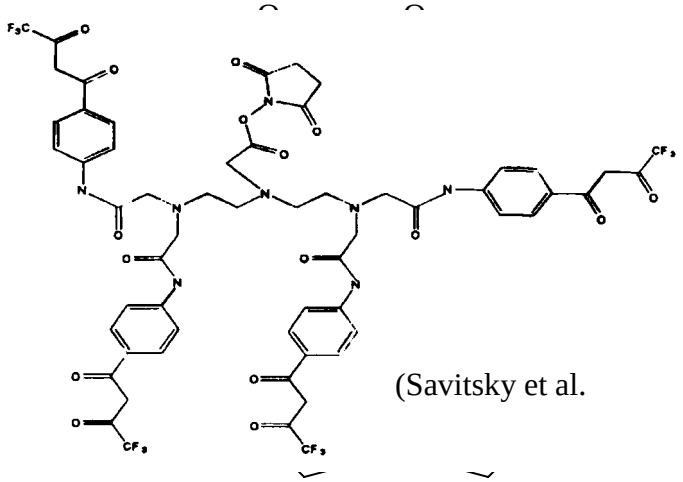

(Savitsky et al.

Cryptates (Lehn, Mathis et al.)

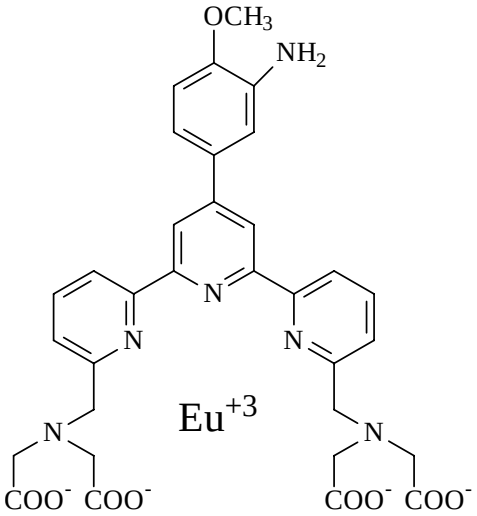

Terpyridine (Saha et al.)

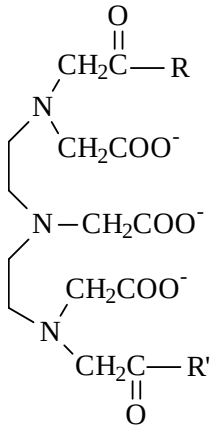

DTPA

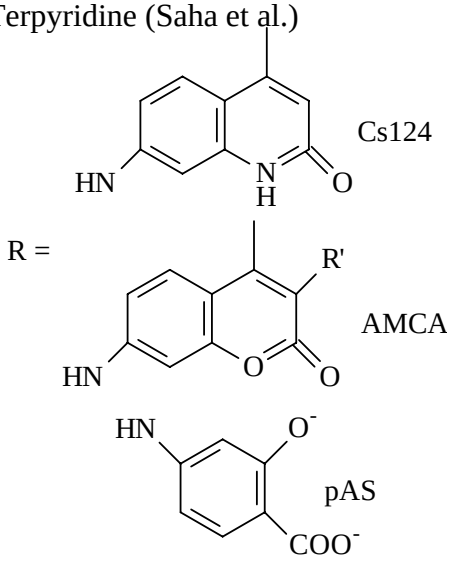

Cs124

AMCA

pAS

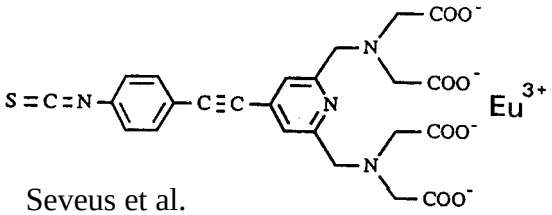

Seveus et al.

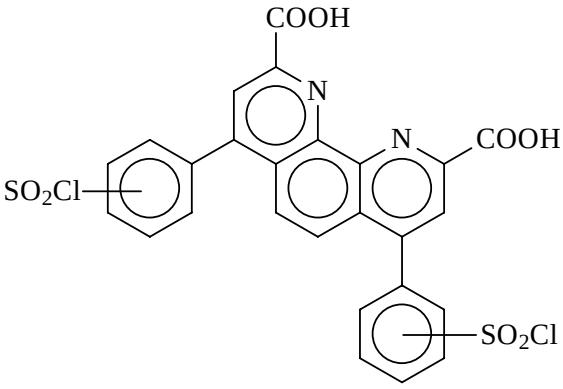

BCPDA

Fig. 2. Representative Emission spectra and Excited-state lifetime. The particular chelate is Tb^{3+}- or Eu^{3+}-DTPA-cs124 (see Fig. 1).

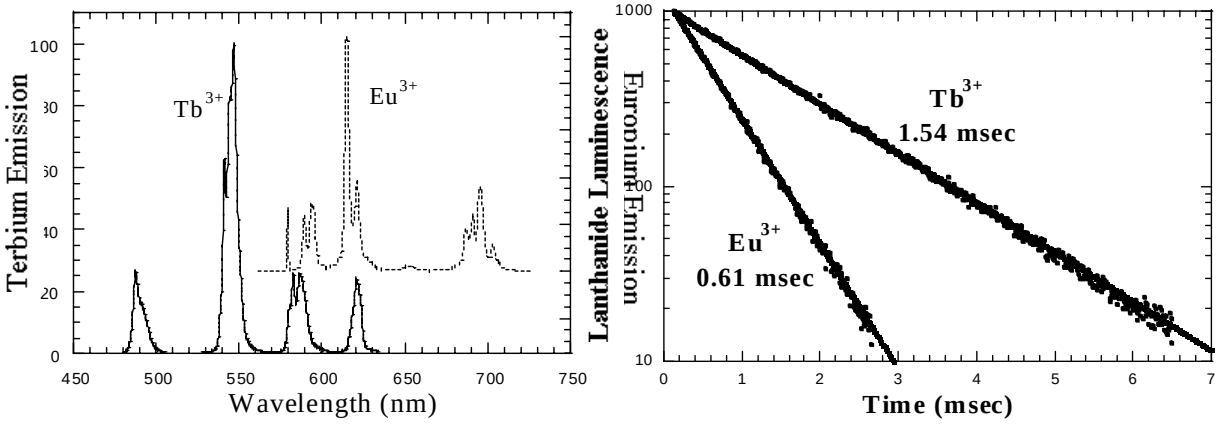

Fig. 3. DELFIA enhancement methodology. A non-fluorescent lanthanide chelate is bound to analyte, and captured on a surface. An enhancement solution releases the Eu which is then bound in a luminescent complex containing a chelate-sensitizer, often napthyltrifluoracetate (NTA), in the presence of triocylphosphine oxide and Triton X-100. The resulting micelle is highly luminescent. From (25).

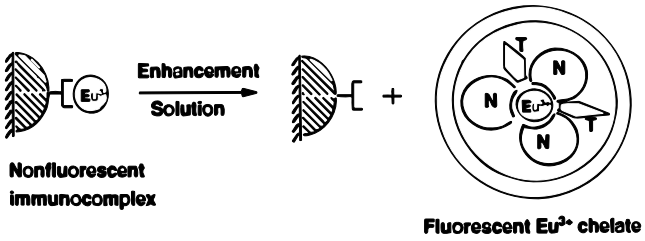

Sensitivity. An important figure of merit when discussing sensitivity is a comparison to radioactive probes. Another benchmark are ELISAs (enzyme-linked immunosorbent assays), the standard clinical assay for antibodies, which have sensitivities in the 10^{-9} to 10^{-11} M range. Detection of a single *conventional* (i.e. organic) fluorophore is feasible if background fluorescence is not a problem, whereas this is not possible for a single radioactive label or antibody in ELISA. (Detection of a single lanthanide probe is highly unlikely because the long-lifetime limits photon flux to below detectable levels.) Hence fluorescence can be orders of magnitude more sensitive than radioactive probes or ELISA assays. However, under many conditions, including those commonly found in high-throughput drug screening applications, radioactivity is more sensitive than conventional fluorophores because contaminating background fluorescence often limits the sensitivity of conventional fluorophores. With lanthanides, however, temporal and spectral discrimination against background fluorescence, which tends to be widely spread in wavelength and nanosecond in duration, is very effective and sensitivities approaching radioactivity are possible.

The lowest detection limit reported for a single chelate is 10^{-15} M but this was in ethanol (100). Among practical systems, the DELFIA system can be quite sensitive, in part because luminescence is achieved in an optimized "enhancement solution". Detection levels of 10^{-12} – 10^{-14} M and 10^{-16} to 10^{-18} moles were reported in immunoassays (82, 99), which compares to roughly 0.05-2 x 10^{-18} moles for radioactivity (52). In DNA studies, Hurskainen et al. detected 5pg (0.15 x 10^{-18} moles or 0.15 attomoles) of lambda phage DNA, labeled with non-fluorescent Eu chelates, by hybridizing to a lambda phage DNA-coated microtiter plate, followed by DELFIA enhancement solution. 7% of total nucleotides were labeled with non-fluorescent Eu chelate introduced by transamination of the DNA, followed by reaction with an amine-reactive chelate. For comparison ^{32}P-labeled lambda phage DNA was hybridized against lambdaphage DNA spotted onto nitrocellulose filter. Hybridization sensitivity was 1 pg after overnight autoradiography at -70 C and 10 pg after Cerenkov counting (counting in liquid scintillation counter without scintillation cocktail). For oligonucleotides (approximately 20mer) end-labeled with about 20 Eu-chelates, DELFIA detection in a hybridization-capture assay led to a sensitivity of 10^7 target molecules, or 17 attomoles (22).

Among directly luminescent chelates, Savitsky et al, in a brief report, claimed equal sensitivity to the DELFIA system (72). The detection limit for the free terpyrdine complex of Saha et al. was reported to be 3 x 10^{-17} moles (presumably in 100 μL, or 0.3pM) and 1.5 x 10^{-16} moles in 100 μL (1.5pM) when bound to DNA (69). Selvin et al. reported 2pM detection sensitivity of free Tb-DTPA-cs124 in an optical system which was not configured for maximum sensitivity (54). Mathis and co-workers detected 2 attomoles of DNA on dot blots with Eu-cryptate, which they stated was similar to other non-isotopic methods (66), and 1 pM of prostate-serum antigen in another Eu-cryptate assay (63). They also compared the sensitivity of Eu-cryptates versus ^{32}P in a DNA-hybridization assay and found them equivalent, although the ultimate detection limit in each case was not reported and conditions of the assay necessarily

differed in the two cases (2). Specifically, they hybridized a cryptate- or ^{32}P- labeled 21-mer to a complimentary biotin-labeled DNA. They then added the ^{32}P labeled DNA to a steptavidin-coated microtiter plate, washed, and read the remaining radioactivity. In parallel they added the cryptate-labeled DNA to a multimeric streptavidin complex bound to a modified allophycocyanine. The cryptate transferred most of its energy to the APC and the time-delayed fluorescence from the APC was measured. (See lanthanide-based resonance energy transfer section below for further discussion.) When using 0.2 pmoles of DNA in 50uL in both cases, they found the same sensitivity. The cryptate has the advantage of being homogenous (requiring no washes) and non-radioactive, but cryptates require 0.4M NaF in the buffer for optimal fluorescence. (Other chelates do not require this.)

Multiple labeling and selected applications. To increase detection sensitivity of biomolecules it is routine to label biomolecules with multiple fluorescent probes. However, organic dyes self-quenching, i.e. the fluorescence intensity increase with the number of labels is less than linear. This is due to the small Stokes shift and possible direct interactions between dyes. Multiple labeling can also reduce the solubility of the labeled biomolecule and adversely affect its function. These factors limit the number of conventional fluorophores attached to an antibody, for example, to approximately 6.

The large Stokes shift and excellent solubility of lanthanide chelates makes multiple labeling of biomolecules possible, although the effect on the biomolecules function is likely application-specific. Takalo et al. showed that an IgG antibody could be labeled with 25 chelates with a linear increase in luminescence (Fig. 4, triangles; circles are intensity per chelate), although antibody activity was not reported (89). Kwiatkowski et al. introduced multiple chelates into DNA via a phosphoramidite technology (48). Dahlén et al. synthesized a series of 14-28 base oligomers with 10, 25, or 40 amino-deoxycytidines on the 5' end, which were then labeled with a europium chelate (22). The 10 and 25 amine-DNA was synthesized in high yield and could be completely labeled, while the yield on the 40 amine labeled DNA was relatively low and could be labeled with a maximum of 26 chelates. In a solid phase assay the melting temperature and hybridization efficiency was unaffected by the chelate tails, although the kinetics were slowed -- not due to the chelates but due to the extra sequence complexity from the addition C's. The linearity of europium fluorescence vs. chelate number was not reported although their data clearly show the oligos with larger number of chelates are brighter. A detection limit of 10^7 oligos was reported, which the authors say is at least as high as other oligonucleotide-based detection systems. Interestingly, on the same 25-chelate oligo, the authors compared the sensitivity when using the directly luminescent europium chelates to the DELFIA method, where the europium was released from the luminescent chelate and then reconstituted into the enhancement solution. Two attomoles (10^6 molecules) in the DELFIA method compared to 10^7 using the directly luminescent chelates was reported.

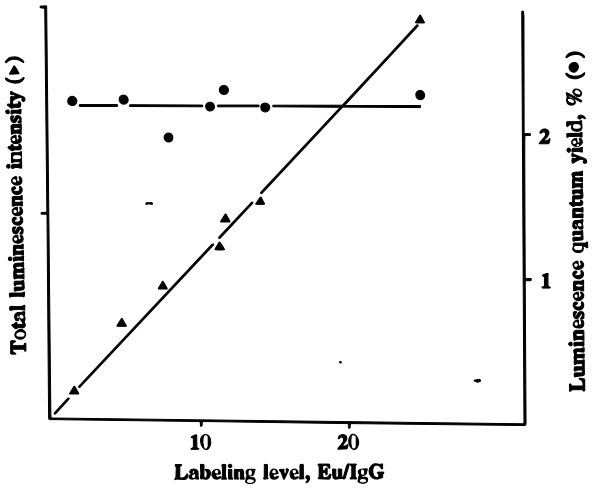

Fig. 4. Multiple chelates can be attached to a biomolecule (antibody) with a linear increase in brightness, in contrast to conventional fluorophores which self-quench.

A common way to minimize adverse effects due to multiple labels is to produce a long tail which contains the chelates and then attach the tail to the biomolecule at only one point. (This method is also used in Magnetic Resonance Imaging with non-luminescent gadolinium chelates to increase contrast and sensitivity (81).) Bailey was the first to report such a method where they used a polylysine tail labeled with over 100 DTPA-paraaminosalicylate chelates, attached at a single point to an antibody (12) (see also Fig. 1). A critical element appears to be complete acetylation of the polylysine to reduce excess positive charge which can lead to loss of function and non-specific staining. Morrone has given a detailed procedure and has well characterized polylyine-DTPA-pAS complexes (64). He showed that 80 Tb chelates could be attached to a polylysine tail which was then attached to a protein (IgG or streptavidin). The protein-chelate complexes were then used to specifically stain cellular organelles, showing that the complexes were functionally active (see Fig. 8 and Imaging section, below). Lamture and Wensel have used polylysine with the chelate-sensitizer dipicolinic acid (51).

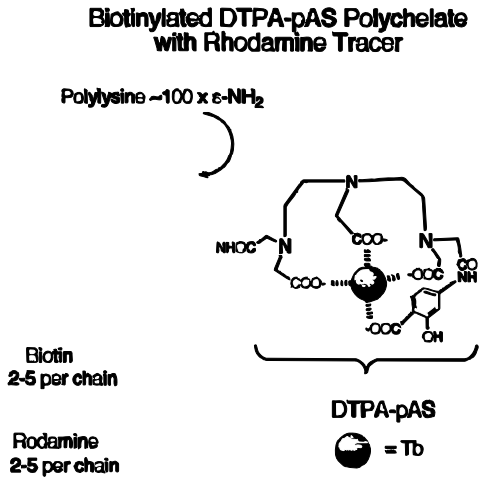

Fig. 5. Multiple chelate-labeling can be achieved by attaching many (10-150) chelates on a polylysine tail, which is then conjugated to a biomolecule at a single point. If conventional fluorophores are also sparsely attached to the polylysine, direct comparison between conventional (including confocal) imaging and time-resolved imaging can be made. (Figure from (64).)

An alternative method for various levels of multiple labeling was reported by Diamandis et. al and commercialized by CyberFluor Inc (Toronto, Canada) under the name FIAgen (reviewed in (25); see Fig. 6). In one version, streptavidin was labeled with approximately 14 BCPDA molecules (see Fig. 1). The sensitivity was 10^{-10} – 10^{-11} M. In a second version, approximately 160 BCPDA molecules was bound to a thyroglobulin cross-linked to streptavidin yielding a detection limit for biotinylated targets of 10^{-11}-10^{-12} M. In a third version, these thyroglobulins were non-covalently bound together, yielding a detection limit of 10^{-12}-10^{-13} M. The complexes were also used in time-delayed imagining studies (60).

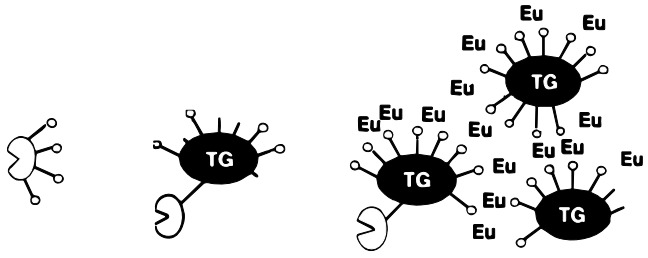

Fig. 6. Multiple BCPDA europium chelates can be incorporated onto streptavidin-thyroglobulin complex (see text for details; figure from (25)).

Yet another method is to use an enzyme-amplification scheme to deposit many labels locally. Tyramide signal amplification (TSA), is a peroxidase-driven amplification system by which a large accumulation of biotin-tyramide is deposited locally, and detected by fluorescently-labeled streptavidin. Signal amplification can be 100-fold. TSA has been used with both conventional fluorophores and with lanthanide in time-resolved detection, the latter being beneficial when autofluorescence is still a problem despite the signal amplification. For example, de Haas et al. used TSA in DNA and RNA in situ hybridization in strongly autofluorescent cells where the biotin-tyramide was detected with europium-labeled streptavidin (24). Signals from the europium labels were sufficiently bright that they could be observed with the eye.

The Diamandis group has pioneered an alternative enzymatic amplification scheme to achieve the low detection limit of 1.5×10^5 analyte molecules in 100 μL, or 2.5×10^{-15} M (17). The general idea is that the presence of an analyte leads to the capture of an enzyme which converts an organic molecule into a sensitizer, leading to lanthanide luminescence. Specifically, an analyte (anti-α-fetoprotein antibody) was immobilized to a surface via a coating antibody. A biotinylated antibody was then added, excess removed, and a streptavidin alkaline phosphatase (ALP) complex added and excess removed. Fluorosalicylic acid phosphate ester (FSAP) was added, which is not a terbium sensitizer, but becomes one when the phosphate is removed by the ALP, forming FSA. The pH is then increased to 13 and Tb-EDTA is added. The Tb-EDTA (without sensitizer or with FSAP) is essentially non-fluorescent, but at pH 13 the FSA can ligate to Tb-EDTA, forming a luminescent complex. The result is that the presence of an analyte leads to many luminescent terbium complexes via the ALP-catalyzed creation of FSA sensitizers. The combination of enzyme amplification and time-resolved detection led to the excellent sensitivity, albeit at a cost of several wash steps. This methodology has been applied to DNA hybridization in both dot-blot and solid-phase microtiter-based assays, achieving detection limits for target DNA of 0.2fmol (16), 125pg (pBR322 DNA; 6×10^{-17} moles) (30) 4 pg (91).

Ioannou and Christopoulos have taken enzyme amplification one further step, combining TSA and ALP amplification to increase the signal by another 30 fold (and the signal to noise by 10 fold) compared to ALP amplification only (46). DNA was immobilized, hybridized to biotinylated DNA, and bound to streptavidin horseradish peroxidase which catalyzed the deposition of biotinylated tyramide to the surface. Alkaline phosphatase-labeled streptavidin was then bound to the immobilized biotin and enzymatically converted the FSAP into FSA as described above.

PCR is of course a very powerful method of DNA amplification and has been used in conjunction with lanthanide luminescence. Diamandis et. al, using, the time-resolved enyzme amplification scheme described, in combination with reverse transcription polymerase chain reaction (RT-PCR) measured prostate serum antigen (PSA) mRNA with high sensitivity: 160 PSA cDNA molecules in the preamplification sample were detected with a signal to background of 10, and mRNA corresponding to one PSA-producing cell in the presence of a million PSA-negative cells was detected with a signal to background of three (33, 34). Sensitive detection of PSA-expressing cells, particularly in the blood and lymphatic systems is important for evaluating

the stage of prostate cancer. (PSA is a 33-kD serine protease glycoprotein are used as a marker for prostate cancer.) Diamandis's method involved using RT-PCR to amplify any PSA mRNA present, with digoxigenin (a hapten)-dUTP used in the amplification step. The denatured amplified DNA was hybridized to a 24mer DNA previously immobilized on a streptavidin-coated microtiter plate via a biotin incorporated at the end of the 24mer. An ALP-labeled antibody to digoxigenin was added and excess removed. Upon addition of FSAP, as described about, the ALP then forms fluorescent terbium complexes which are detected in time-resolved mode.

PCR and the DELFIA method have also been combined. For example, PCR in combination with DELFIA detection system was capable of detecting a single purified coxsackievirus A9 RNA from clinical samples (36); 5 copies of HIV-1 DNA (21); 50 prostate serum antigen mRNAs and a single PSA mRNA expressing cell (101). In the latter case, to enhance sensitivity, oligonucleotide probes for PSA mRNA contained 20 chelates at the end. PCR and the DELFIA methodology have also been combined to detect point mutations (21, 45).

One of the more interesting applications of PCR and lanthanide luminescence is a seven pseudo-color assay utilizing the DELFIA system to detect human papilloma virus (HPV) types. This application takes advantage of the sharply-spiked spectra of lanthanides, which leads to very little spectral overlap when using more than one lanthanide, and the ability to excite multiple lanthanides with single excitation wavelength. (70). HPV infection is implicated in cervical and other cancers. The cancer risks are correlated with HPV type, and hence detection of HPV type is important. The general scheme is outlined in Fig. 7. PCR was used to amplify a portion of the HPV containing type-specific sequences and to introduce a biotin which was then used to immobilize the amplified DNA on a streptavidin-coated solid support. DNA probes specific to HPV type and containing 10-20 (non-fluorescent) chelates labeled with a unique combination of Eu, Tb or Sm were then hybridized to the target DNA. (This combinatorial approach has been used with great success with regular probes as well (67, 86).) After free probes were washed away, an enhancement solution was added and Eu, Tb and Sm luminescence was measured at 615 nm, 545 nm, and 642 nm with various time delays. For the Eu-labeled probes, 100 amol of target DNA could be detected, with lower poorer sensitivity with Tb and Sm. All seven type of HPV strain were correctly identified. The group has also applied this technology to the detection of diabetes-related HLA alleles (83).

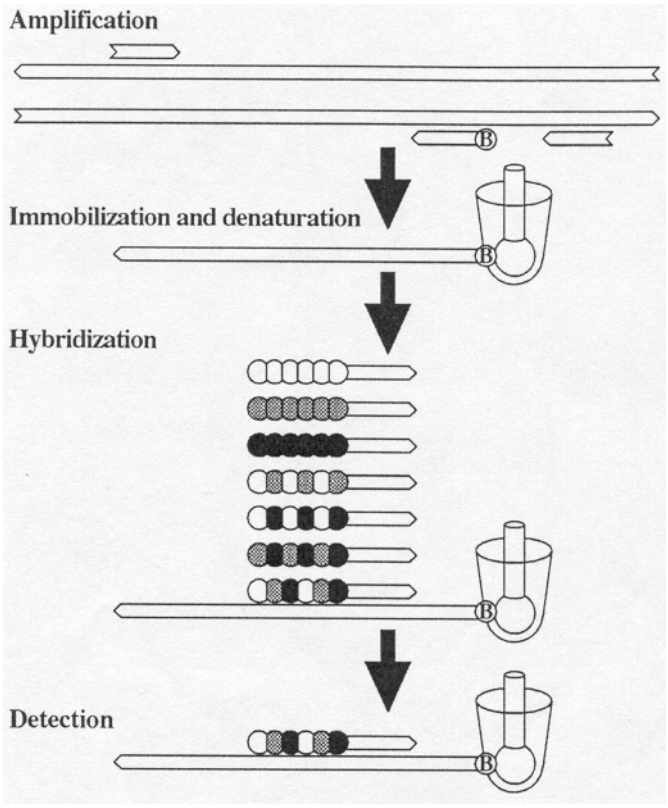

Fig. 7. Methodology for 7-pseudo color detection of multiple human papilloma virus types using PCR amplification and multiple lanthanide chelates. See text for details. (Figure from (70).)

Imaging

One of the most demanding applications of lanthanides is in imaging. In scanning microscopy, the slow emission rate of lanthanides greatly slows data acquisition: with a millisecond lifetime, it is necessary to wait at least this long on each pixel, leading, for example, to an acquisition time of over 5 minutes for a 500 x 500 image. Nevertheless, Morrone used scanning x-ray microscopy to take very high resolution (75 nm) images of lanthanides specifically labeled in cells (64). To increase signal levels, Morrone used a terbium-loaded polylysine tail (see above), which also contained trace rhodamine (or fluorescein). Importantly, this dual-label approach enabled him to correlate the images obtained with x-ray excited terbium luminescence to confocal images of rhodamine emission and showed that they were essentially identical, except for the higher resolution afforded by the x-ray excitation. Although the published figures where for the proteins actin and tubulin (Fig. 8a), similar results were achieved using FISH (Fig. 8b,c), splicing factor (a protein involved in removal of introns and splicing of mRNA form exons) and NuMA (nuclear mitotic spindle apparatus, a protein needed in cell division) (personal

communication). These latter examples are particularly important because labeling is within the nucleus where non-specific labeling can be the most troublesome because trivalent lanthanide can bind directly to DNA if they are pulled out of their chelate.

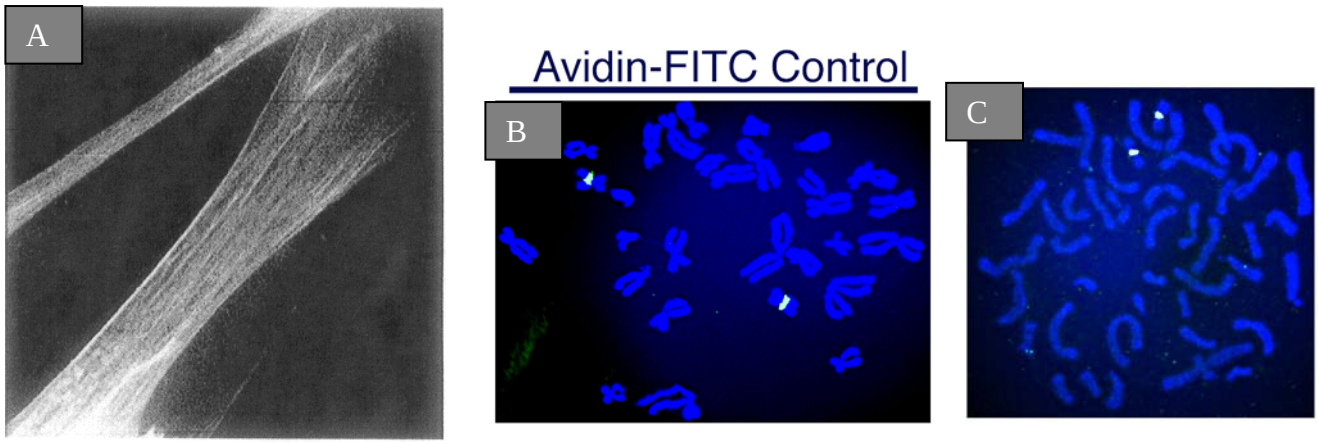

Fig. 8. Specificity in labeling can be achieved with multi-chelate complexes. (a) Actin fibers in a Wi38 fibroblast cell labeled with biotinylated phalloidin, followed by streptavidin and a biotinylated polylysine-chelate containing approximately 80 chelates. Terbium luminescence was stimulated by soft x-ray excitation. (b) FISH using conventional fluorescein-labeled probes – a control for (c). (c) FISH using poly-chelate Tb probes containing trace rhodamine and visualized by exciting and detecting rhodamine fluorescence, similar to (b). A comparison of (b) and (c) shows that the polychelate probes are capable of specific hybridization to their target.

In wide-field imaging, lanthanides and time-resolved detection can be used to great advantage in samples where autofluorescence reduces contrast with conventional probes (5). Pulsed excitation and time-delayed detection is used to discriminate against the autofluorescence, which tends to be nanosecond in duration. The time-delay can be achieved with a chopper (59, 60), ferroelectric liquid crystal shutter (90, 93), an image-intensified CCD (39), or possibly in the near future with CCDs containing an electronic shutter. The slow emission rate of the lanthanides still precludes rapid acquisition times, but in wide-field imaging acquisition times of tens of seconds may be acceptable.

Periasamy et al. detected a Eu-labeled FISH (fluorescence in situ hybridization) probe against human papillomavirus (HPV) 16 DNA (65). The use of long-lived probes in such application is particularly advantageous for FISH on standard PAP smears which have already been stained with conventional absorption dyes used by pathologists because these dyes tend to be highly autofluorescent and obscure FISH signals when using conventional fluorescent dyes.

Fig. 9 show the images without and with time-delayed detection, where the latter dramatically increases contrast. In both cases excitation was in the UV. A more realistic comparison is to compare lanthanide probes (necessarily excited in the UV) using time-resolved detection with conventional fluorescent dyes excited in the visible without time-resolved detection. Seveus et al. made such a comparison for europium- and fluorescein- labeled streptravidin bound to biotinylated antibodies to a human colon cancer antigen (79). The cells were highly autofluorescent due to glutaraldehyde fixation in a permanent mounting medium. Integration times of 10 seconds for the europium in time-resolved mode and 0.5 seconds for the fluorescein in prompt (conventional) mode led to similar signal strengths – 16,000 for europium and 12,000 for fluorescein – but the background with europium was near the detector noise (5 counts per pixel), whereas with fluorescein the autofluorescent background was approximately 2000 counts. Hence the signal/background with europium was over 3000:1, whereas with fluorescein it was 6:1, or a 500-fold improvement using time-resolved detection of europium. An earlier paper by the same authors reported more modest gains when using time-resolved imaging of europium chelates in FISH for the detection of collagen mRNA and human papillomavirus sequences (80). The limitations of this earlier work appeared to be due to a chelate which was not very photostable. More recently other workers have used time-resolved imaging of a europium chelate to image prostate-serum antigens where they state that photostability was not a problem (6). Future applications of time-resolved imaging in FISH and other areas using lanthanides in samples which are highly autofluorescent look promising, although very low target number will likely require amplification schemes due to the inherently low intensity (long lifetimes) of the lanthanides.

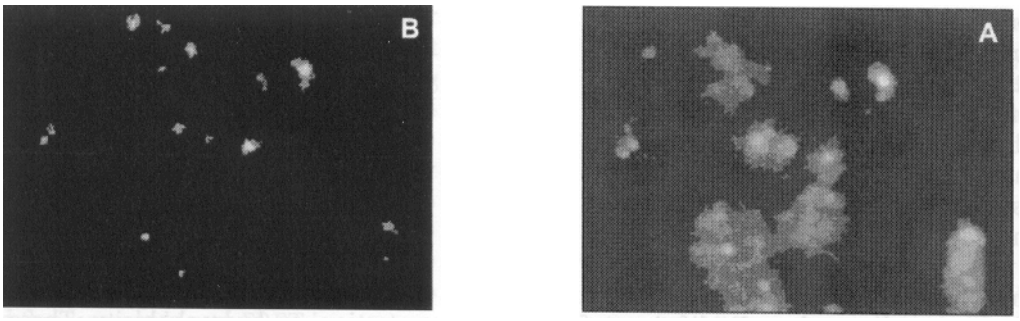

Fig. 9. Comparison of time-resolved (left) and conventional, i.e. prompt or steady-state fluorescence image of HPV DNA in fixed CaSki cells. The contrast is greatly enhanced by time-resolved detection (30 μsec delay after pulsed excitation with a window of 250 μsec). CaSki cells contained approximately 500 copies of HPV. 8kB DNA probes were labeled with biotin-11-dUTP via random-priming method and after hybridization to target, europium-conjugated avidin (Wallac Inc.) was added.

Alternative time-resolved probes. As mentioned, the millisecond lifetime and sharply spiked spectrum of lanthanides are highly advantageous for discriminating against background fluorescence. However, the long lifetime limits emission rate. To date, lanthanides also require UV excitation, which is particularly disadvantageous in microscopy. When this is an issue, microsecond dyes are attractive alternatives. Tanke et. al and Savitsky et al. have developed an impressive set of Pd and Pt porphoryn-based probes which appear to be unusually bright with many favorable spectral characteristics: extinction coefficients up to 200,000 $M^{-1}cm^{-1}$ with an excitation peak at 380 nm and a smaller peak in the visible (530 nm), emission in the red (> 650 nm), and quantum yields ranging from in approximately 0.1-0.3 (58, 90). They have used the porphyrins in FISH and many other systems (90). The primary disadvantage of the system is that the porphyrins used are hydrophobic, they require deoxygenation for maximal emission, and the chemistry of coupling to biomolecules is not straightforward. (Tanke et al. have developed an amine-reactive NHS ester (23), although a thiol-reactive porphoryn has not been reported.) Lakowicz et al. has published many papers reporting microsecond dyes based on Ruthenium, rhenium, and Osmium. These probes can be excited in the visible to red, be highly polarized, and have pM sensitivity **JOE: DO YOU HAVE A REFERENCE OR REFERENCES FOR PICOMOLAR SENSITIVITY?**A review has recently been written summarizing this work (50).

Lanthanides as donors in resonance energy transfer.

Fluorescence resonance energy transfer (FRET) is a widely used technique to measure the distance between two points which are separated by approximately 10-100 Å. A number of excellent reviews on FRET have been written (13, 18-20, 29, 31, 40, 74, 88). Lanthanide-based RET (LRET) is a recent modification of the technique with a number of technical advantages, yet relies on the same fundamental mechanism — subject to careful interpretation of various terms. A recent review of LRET has appeared (75), as well as a summary of lanthanide luminescence (8) and its application in biology (71, 76). LRET has primarily been applied to proteins (7, 9, 61, 62, 68, 87, 95, 98), although there have been a number of applications to DNA (14, 41-43, 55, 77, 78). Here we provide a brief summary of the relevant theory before highlighting some LRET applications to DNA.

In FRET, an excited fluorescent donor molecule attached at one point in the biomolecule, transfers energy to an acceptor molecule attached at a second site, through a non-radiative dipole-dipole coupling which is inversely proportional to the sixth-power of the distance between the two dyes:

$$E = 1/[1+ (R/R_o)^6] \quad (1)$$

E is the efficiency of energy transfer from donor to acceptor, i.e., *E* is the probability that an excited donor will transfer its energy to the acceptor instead of decaying via other pathways such as fluorescence or heat. R_o is the distance at which half of the energy is transferred and is generally 20-50 Å, although can be ≥ 70 Å when using lanthanides and ≥ 80 Å with far-red dyes (73). R_o depends on the spectral properties of the donor and acceptor and also on their relative orientation. (The orientation dependence of R_o, is often referred to as κ^2. This can be a significant source of uncertainty in determining distances via FRET – see below under advantages of LRET.) By knowing R_o, which can be calculated or experimentally determined, and measuring *E*, the distance between the probes can be found. *E* can be measured because it reduces the donor's intensity and excited-state lifetime:

$$E = 1 - I_d/I_{da}, = 1 - \tau_d/\tau_{da} \qquad (2)$$

where subscript refers to donor's intensity or lifetime in the absence (I_d, τ_d) and presence of acceptor (I_{da}, τ_{da}). *E* can also be measured by comparing the amount of fluorescence from donor and from sensitized emission of the acceptor, i.e. the acceptor emission due only to energy transfer from the donor.

$$E = (I_{ad} / Q_a) /(I_{da} / Q_d + I_{ad} / Q_a) \qquad (3)$$

where I_{da} is the integrated area under the donor emission curve in the presence of acceptor, I_{ad} is the integrated area of the sensitized emission of the acceptor (i.e., not including the fluorescence due to direct excitation of the acceptor, which may occur when exciting the donor) and Q_i is the quantum yield for donor or acceptor.

Advantages of LRET

We and others have shown that using luminescent terbium or europium chelates as donors and organic-based acceptors, yields many technical advantages over conventional FRET (54, 61, 62, 74, 75, 77, 78). Terbium can readily transfer energy to dyes such as fluorescein, tetramethylrhodamine, Cy3, and Alexa dyes, while Europium can transfer energy to Cy5 or allophycocyanine.

An example which highlights these advantages is shown in Fig. 10, where energy is transferred from a europium chelate attached at the 5'end of a DNA oligomer to an organic dye (Cy5) at the 5' end of a hybridized strand. Fig. 10a shows energy transferred measured spectrally. Pulsed excitation, followed by detection after a delay of approximately 100 μsec is used to eliminate any prompt fluorescence, including direct excitation of the acceptor. Hence, any emission of the acceptor is due only to energy transfer from the (long-lived) donor. The donor-acceptor spectra displays a large peak around 670 nm which is the Cy5 sensitized emission. The signal to background is excellent because the donor is silent in this region and

direct acceptor emission is eliminated. Indeed, the background is largely due to detector noise, which can be made extremely small with modern detectors.

Figure 10b shows the same system where energy transfer is measured temporally, following an excitation pulse. The europium donor-only is single exponential with 2.5 msec lifetime. Sub-stoichiometry amounts of a Cy5 labeled complementary DNA was then added. Upon hybridization, the Eu^{3+} decay becomes bi-exponential, indicating two populations of donors. One is essentially unquenched (lifetime 2.4 msec) which is the europium not hybridized to a Cy5-strand. The other is highly quenched (lifetime 0.22 msec; $E = 1 = 0.22/2.5 = 0.91$), corresponding to a Eu-DNA hybridized to Cy5-DNA. (A control of Eu-DNA hybridized to an unlabeled strand shows no quenching.) The Eu-DNA-Cy5 complex leads to sensitized emission of Cy5, whose lifetime can be measured at 668 nm. This lifetime is determined by the lifetime of the Eu-donor "feeding" the Cy5. The 0.25 msec of the sensitized emission is in good agreement with the 0.22 msec Eu-lifetime component measured by donor-quenching. Note that even though a mixture of donor-only and donor-acceptor is present, the sensitized emission lifetime only arises from the donor-acceptor complex. This has important implications for systems where labeling is incomplete or unknown.

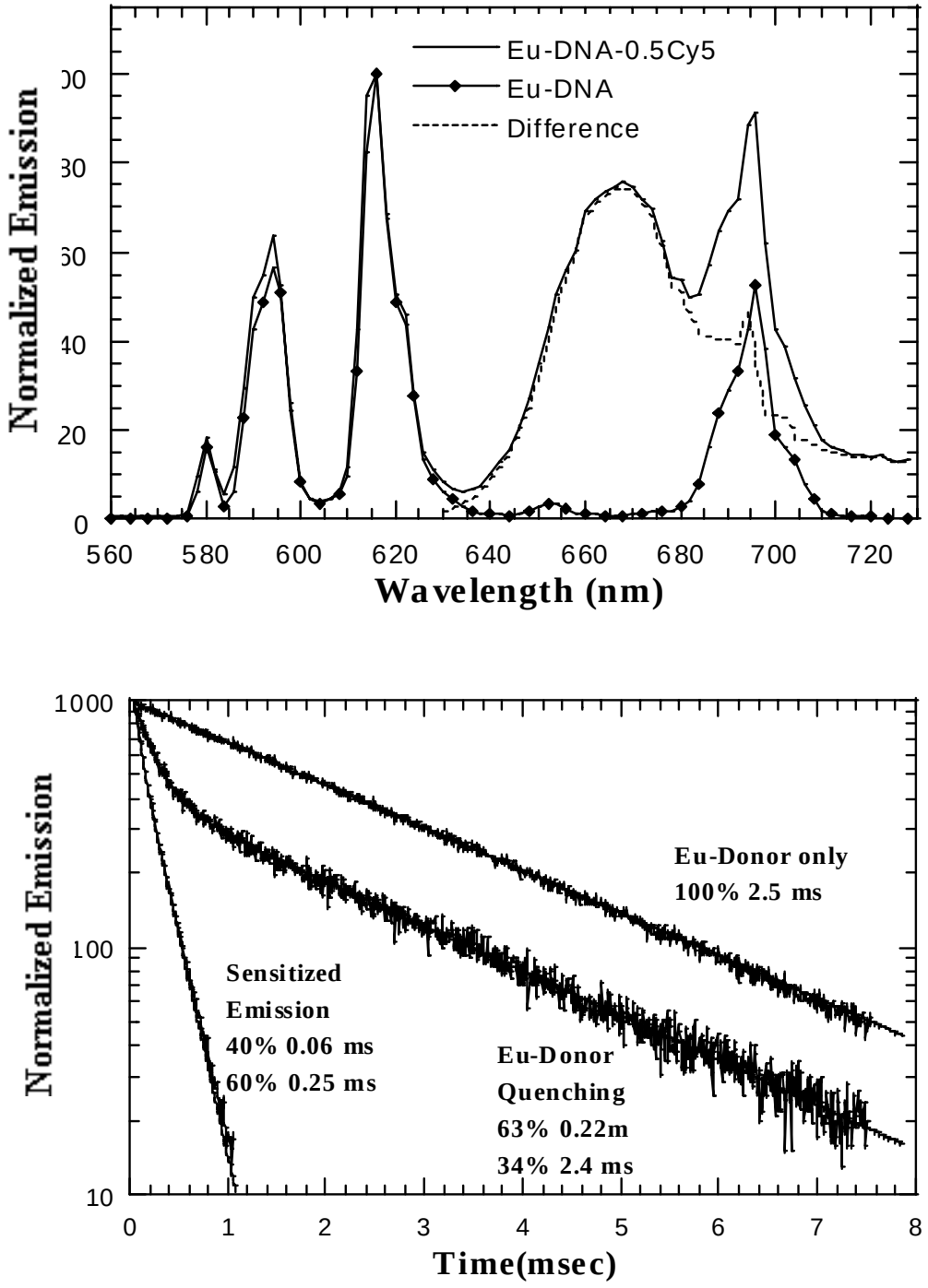

Fig. 10. Time resolved (a) and spectral (b) measurements of LRET from a Europium donor to a Cy5 acceptor on a 10mer DNA. See text for details. Adapted from (78).

The advantages of LRET, compared to conventional FRET which relies on two organic fluorophores, are the following:

• The efficiency of energy transfer using lanthanides as donors is considerably higher compared to most organic-based donors, leading to larger signals and farther measurable distances. The R_0 is typically 50-70Å with current chelates, and as high as 90 Å with allophycocyanin as the acceptor. This is larger than most conventional FRET pairs. In addition, the R_0 can be optimized to the particular system by varying the amount of H_2O/D_2O because D_2O increases the lanthanide quantum yield (44), thereby changing R_0. Lastly, the lanthanide quantum yield is insensitive to pH over a wide range (pH 5-9) and hence, these R_0s are maintained over a wide pH range if the appropriate acceptor is used.

• In LRET, energy transfer is primarily dependent on the distance between donor and acceptor, and not on their relative orientation, leading to more precise distance measurements. This is because donor Tb^{3+} emission is inherently unpolarized and hence donor orientation does not affect energy transfer efficiency (84). Eu^{3+} can be polarized (92) but is often unpolarized when attached to biomolecules via conventional and relatively flexible linkers. With the donor emission unpolarized, κ^2 is constrained to be between 1/3 and 4/3, the extreme cases corresponding to a completely rigid acceptor or perpendicular or parallel to the radius vector, respectively. (In FRET, $0< \kappa^2 < 4$, where $\kappa^2 = 0$ leads to $R_o = 0$ and hence no energy transfer at any distance.) If one then assumes $\kappa^2 = 2/3$, as is often done (donor and acceptor both unpolarized), then at most the distance inferred is in error by +/-12% (75, 88).

• Because of the donor's unusually long lifetime (msec), LRET lifetime measurements can be made with high precision: lifetime measurements avoid problems of concentration determination and allow analysis of heterogeneous mixtures. The long-lifetime also means it is likely that the donor's and acceptor orientation is unpolarized because they have a millisecond to reorient, rather than the nanoseconds typical of organic lifetimes.

• In LRET, a 50 to 100-fold improvement in signal to background of the sensitized emission compared to conventional FRET has been achieved, largely through the reduction of background. In particular, the acceptor's sensitized emission can be measured with no background, either from donor luminescence or from direct excitation of the acceptor. Specifically, the emission of the acceptor due to excitation by the excitation light, which has nanosecond lifetime, is discriminated against using pulsed excitation and time-delayed detection. The donor emission is discriminated against by wavelength filtering — donor emission is highly spiked, with regions of darkness (see Fig. 2) and with the appropriate choice of acceptor, acceptor fluorescence is in this dark region. The improvement in signal to background enables long-distances to be measured (where the signal is weak), and easier handling of incompletely-labeled samples (because excess acceptor or donor do not contribute background).

• In LRET, the lifetime of the acceptor decay due to energy transfer, i.e., sensitized emission, can be measured (see "sensitized emission" lifetime curve in Fig. 10b). This decay follows the donor's lifetime because it is being "fed" by the long-lived donor, which is the rate-limiting step. As soon as the acceptor receives a quanta of energy from the donor, it will, within its

nanosecond lifetime, emit that energy as an emission photon. The ensemble decay of many such acceptor molecules is a signal at the acceptor's emission wavelength which decays with the donor lifetime in the donor-acceptor complex. The sensitized emission lifetime is insensitive to concentration, *and arises only from the fully labeled donor-acceptor complex*. Hence if there is incomplete labeling, with some biomolecules labeled only with donor or only with acceptor, these do not contribute to the sensitized emission signal. This significantly increases the number and type of samples which can be looked at with resonance energy transfer since complete labeling is often not possible and leads to difficulties in conventional FRET.

A description of an instrument optimized to perform LRET has been described recently (96). A schematic of the instrument is shown in Fig. 11. There are several commercially available instruments (Perkin-Elmer Corp., Norwalk Ct.; Packard Instruments, Meriden, CT; Spex-Instruments SA, NJ; Wallac, Gaithersburg, MD; Cis Bio International, Cedex France) which are capable of making micro- to millisecond time-resolved fluorescence measurements used in LRET.

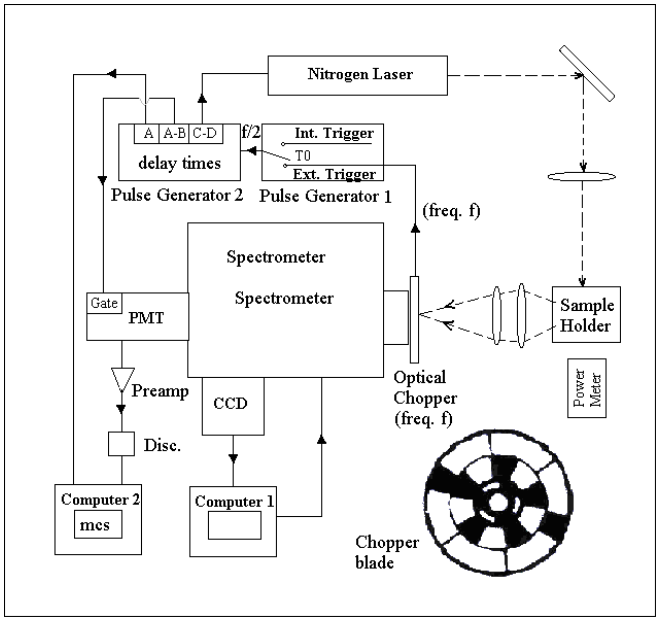

Figure 11. In LRET, a pulsed nitrogen laser (l = 337 nm, 5 nsec full-width-half-max, 40-50 Hz repetition rate) excites the lanthanide chelate which then emits and/or transfer energy to an acceptor which also emits. An optical chopper directly in the detection pathway is timed such that all prompt fluorescence is eliminated. The spectrometer spreads the emitted light by wavelength and the light is detected either by a CCD to obtain an emission spectra with all wavelengths collected simultaneously, or by a photomultiplier tube which is connected to a multi-channel scalar to acquire time-decay of donor or acceptor (sensitized emission) luminescence at a particular wavelength, with 2 microsecond resolution. See (96) for more details.

LRET applied to protein – DNA interactions.

Protein-induced DNA bends. The Heyduk lab has been very active in using LRET to study DNA-protein interactions. In one of their earlier works they used LRET to measure protein-induced DNA bending (Fig. 12) (43). The bending of DNA is essential to the packing of DNA into chromosomes, and is often involved in transcriptional regulation as well. Electrophoretic gel-shift assays are widely used to determine if a particular protein bends DNA – bent DNA runs differently in the gel than straight DNA. However, LRET has a number of advantages, albeit at a cost of greater experimental complexity. In particular, LRET is a relatively direct measure of DNA bending and can be accomplished under a wide variety of solution conditions, including moderate to high salt conditions not attainable in gels. LRET, unlike FRET, is also capable of measuring the requisite distances, which can be up to 100 Å.

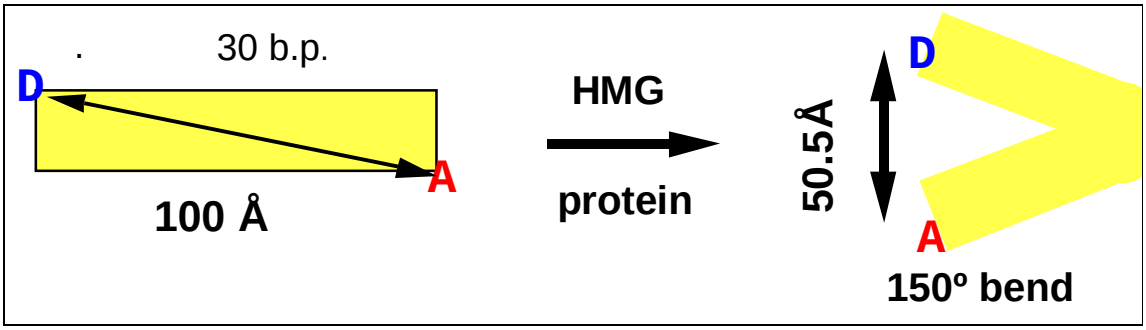

Fig. 12. Some proteins, such as high mobility group proteins, can bend DNA. This can then be detected via LRET because the end-to-end distance changes. (Adapted from (43).)

The Heyduk lab studied DNA bending induced by a class of proteins known as high-mobility-group (HMG) proteins. Except for the histone proteins, which bend DNA into sharply curved structures called nucleosomes, HMG proteins are the most abundant proteins associated with chromatin. One subset of HMG proteins binds to DNA with high affinity at specific sequences, and a second subset binds with relatively little specificity (aside from binding to A-T rich regions). A number of the sequence-specific HMG proteins have been shown to sharply bend DNA when bound to their high-affinity site, but before the Heyduk and co-worker's paper, only indirect evidence existed that sequence non-specific HMG proteins bent DNA.

The authors end-labeled complementary 30-base pair strands of DNA, one with a europium donor chelate, and the other with the acceptor dye Cy5. The idea is that in the absence of bends, the DNA adopts its normal B-form configuration and is therefore straight. The donor-acceptor distance is then approximately 100Å (3.4 Å per base along the helix axis, and secondarily, a

helix diameter of approximately 15 Å). In this case the donor-only lifetime was 603 +/- 2 μsec and the donor-acceptor lifetime was 586 +/-3 μsec, corresponding to 2.7% +/- 1% energy transfer or a distance of 100 Å +/- 10 Å. Note that because the donor-only lifetime was rigorously single exponential, the lifetimes could be measured very accurately, and hence, even this small amount of energy transfer could be measured. Upon addition of a protein that bends the DNA, the ends come considerably closer, measured to be 50.7 Å +/- 1.5 Å from a Eu lifetime of 226 +/-22 μsec, or 62% +/- 4% energy transfer. Fig. 13 is representative data showing that as more protein is added and binds, a greater fraction of the DNA is bent, resulting in a larger fraction of the europium that is quenched. The longer lifetime (544-585 μs) is from Eu on unbent DNA (with Cy5 on the complementary strand); the shorter component (200 μs) is from DNA which is bent by the cHMG protein. There is good agreement between the short component of the donor lifetime and the sensitized emission lifetime.

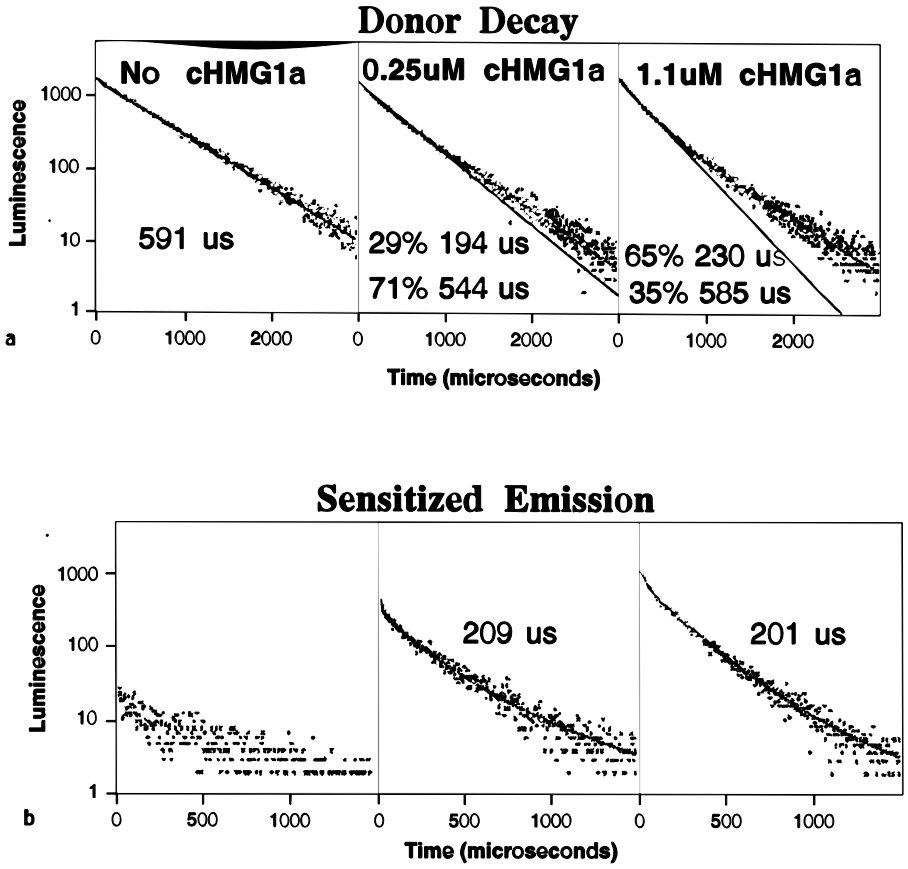

Fig. 13. The Europium donor, hybridized to a Cy5-containing complementary DNA is bent by HMG protein. The donor decay displays two components, a long-component corresponding to unbent DNA (from protein-free DNA) and a short component from bent DNA (from protein-bound DNA). This can be measured either by donor lifetime quenching (top panel) or sensitized emission (bottom panel). Adopted from Figs. 3 and 4 of (43).

More recently, Heyduk and co-workers have used LRET to study conformational changes and the architecture of macromolecular complexes involved in transcription initiation in prokaryotes (10, 42). The first step in transcription initiation in prokaryotes involves recognition of promoter DNA sequence by a multisubunit enzyme RNA polymerase (reviewed in (37)). One of the subunits, σ^{70}, is involved in the initial recognition of the promoter DNA via direct protein-DNA contacts separated by ~ 17 base pairs. σ^{70} exits in the cell in two major forms: free and in complex with the remaining RNA polymerase subunits (core polymerase). However, only σ^{70} in complex with the core RNA polymerase is able to specifically recognize promoter DNA while

the free σ^{70} does not bind to promoter DNA. Thus, the promoter recognition capabilities of σ^{70} are allosterically regulated by an interaction of σ^{70} with the core polymerase.

LRET experiments were used to investigate the nature of the regulation of σ^{70} promoter DNA binding activity (10). The idea was to look for conformational differences in σ^{70} in the bound and free form which might affect its DNA recognition ability. The specific incorporation of the donor (DTPA-Eu-DTPA-AMCA-maleimide) (41) and the acceptor (Cy5 maleimide) into selected domains of σ^{70} was achieved by preparing a set of σ^{70} mutants with pairs of unique reactive cysteine residues engineered into the desired locations. Since both donor and acceptor were thiol-reactive, and both labeling sites were sites were cysteine residues, a mixture of donor-donor, donor-acceptor, and acceptor-acceptor labeling resulted. However, by using LRET, the sensitized emission arising from only the donor-acceptor complex could be measured. Good quality determinations of τ_{ad} were possible in this case even though the donor-acceptor species constituted only approximately 25% of the mixture. Representative LRET data is shown in Fig. 14. It would be difficult to perform these measurements with FRET utilizing classical fluorescence probes.

Comparison of distances measured for the free σ^{70} and the core-bound σ^{70} revealed that most distances were very significantly increased upon binding of σ^{70} to the core polymerase. (DNA was not present in these experiments since σ^{70} binding to the core polymerase is not DNA-dependent.) (See Fig. 14.) One of the distances measured, between residues 442 and 366, allowed a direct comparison between a distance measured by LRET in solution and a distance between the same residues measured in the crystal since both of these residues were present in a σ^{70} fragment for which a crystal structure is now available (57). An excellent agreement between these distances was found – 35Å in the crystal structure vs. 38 Å measured via LRET – providing a further validation of LRET results. In total six distances between four sites in the σ^{70} protein were measured, making it possible to build three-dimensional models of the architecture of σ^{70} protein domains in free and core-bound protein.

Fig 14. The effect of core RNA polymerase on σ^{70} measured by sensitized emission lifetime. Thiol-reactive Eu donor and Cy5 acceptor were labeled at positions A59C to R596C in σ^{70} and sensitized emission of free and core-bound σ^{70} was measured. The increase in sensitized

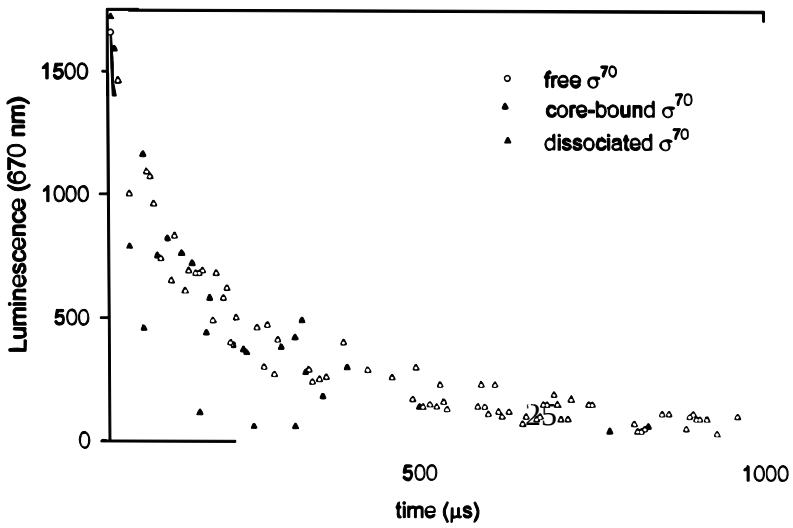

emission lifetime upon core-binding indicates less energy transfer and an increase in distance between these sites. From Fig. 3D of (10).

These models revealed that an interaction of σ^{70} with the core polymerase induced repositioning of DNA binding domains of σ^{70} and the movement of N-terminal domain away from the DNA binding domains. These results provided thus a structural rationale for understanding the core-induced changes in DNA binding properties of σ^{70} protein and were consistent with previous mutagensis experiments which suggested that σ^{70} promoter DNA binding activity is inhibited in free σ^{70} by the N-terminal domain of the protein. The regulation of DNA binding activity of σ^{70} by the core polymerase involves both "unmasking" the DNA-binding domains by the N-terminal domain of the protein and the repositioning of DNA binding domain such that in core-bound σ^{70} they have a spacing compatible with simultaneous interaction with promoter elements separated by ~ 17 bp DNA.

The Heyduk lab later went on to use LRET to measure distances between five sites in σ^{70} and both the 3' and 5' ends of bound DNA (42). The LRET experiments were performed to obtain information regarding the architecture of the nontemplate ss DNA-σ^{70} complex (42). Energy transfer, as measured by donor decay and sensitized acceptor signal were easily detected in the presence of acceptor-labeled oligonucleotide in the case of core-bound σ^{70} while no detectable energy transfer was observed in the case of free σ^{70} (as expected, since free σ^{70} does not bind DNA). LRET experiments were performed with all combinations of donor-labeled core-bound σ^{70} subunit and acceptor-labeled oligonucleotides. Thus, 10 distances were measured which allowed building a model of a complex between ss DNA and the σ^{70} subunit. This model revealed that ss oligonucleotide was bound with a defined polarity and was located across the α-helix containing regions of σ^{70} indicated by mutagenesis as important for σ^{70} function.

New DNA dyes based on LRET with tuneable emission color and excited-state lifetime.

One of the most important applications of fluorescence is simply the detection of fluorescently labeled targets. Multi-color fluorescence is widely used in biosciences for the simultaneous or sequential detection of multiple targets. Using conventional techniques, approximately five different colors can be detected on a single sample, and by using combinatorial methods, detection of more than two-dozen pseudo-colors on a single sample has been achieved (86). Multi-lifetime fluorescence is another possible method for discrimination of signals (32). However, the excited-state range of organic-based fluorophores is limited, generally in the 1-10 nsec range, and not systematically tunable. Metal-chelate complexes can extend the lifetime regime to microseconds (49), and lanthanides, as we have seen, can have millisecond lifetimes (8). As previously mentioned, these long-lived probes have the advantage that background fluorescence, which is typically nanosecond in lifetime, can be readily discriminated

against. Another advantage is that instrumentation is considerably simpler in the micro- and millisecond time regimes than in the nanosecond regime. However the number of long-lived luminescent probes is limited, and millisecond probes have inherently limited emission rates (≈1000 photons/sec/molecule).

Recently it has been shown that using compound dyes in which a fluorescent donor molecule transfers energy to a nearby acceptor dye can yield enhanced emission characteristics including a single excitation wavelength and multiple emission wavelengths (4, 35). These dyes have been particularly useful for improving sensitivity in DNA sequencing applications (47). In principle these dyes can be used with any biomolecules, although in practice, they have been limited to DNA-binding dyes because the DNA provides a very convenient and robust scaffold for placing the donor-acceptor at well defined positions. These dyes relied on organic fluorophores having excited-state lifetimes in the nanosecond range, and hence enhanced lifetime characteristics have not been shown.

Very recently, we have reported on the development of compound dyes using a long-lived lanthanides as donors and a conventional organic fluoropohores as acceptors (Fig. 1). These compound dyes have both tunable emission wavelengths, from 520-680 nm, and simultaneously tunable excited-state lifetimes, ranging from 50-500 μsec (14). Future work is expected to extend these ranges yet further. We call these lifetime and color-tailored fluorophores (LCTF). By utilizing both the time-domain and wavelength-domain, these probes have the potential for quadratically increasing the number of detectable probes on a single sample.

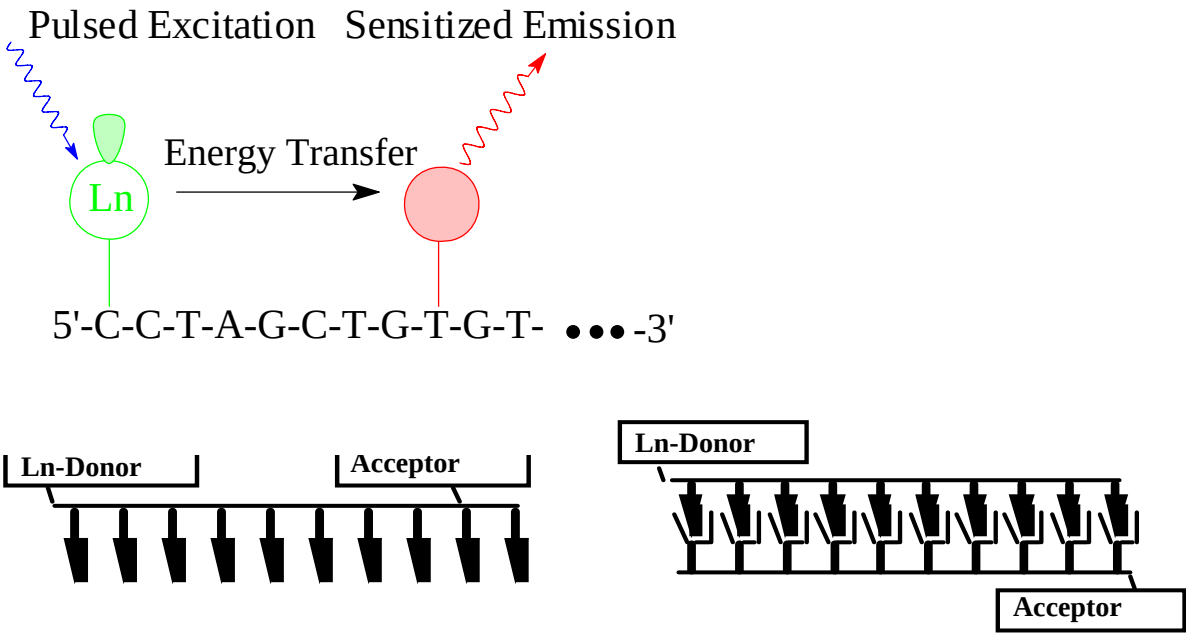

Fig. 15. General outline for construction of lifetime- and color- tailored fluorophores based on a long-lived lanthanide chelate transferring energy to a conventional fluorophore. The probes can be attached to DNA on the same strand or on complementary strands, at the end or in the middle.

To construct an LCTFs, a lanthanide donor molecule (lifetime $\tau_o \approx$ msec in the absence of acceptor) is placed a defined but controllable distance from an organic acceptor fluorophore. The lanthanide transfers energy to the acceptor, which then re-emits (Fig. 15). The color and lifetime of this re-emission i.e., the sensitized emission, are tuneable. The color is tuneable because, when energy transfer (E) is chosen to be large, emission color is largely determined by the acceptor fluorophore, which can be chosen for the desired emission color. The lifetime of the complex is tuneable because it is determined by the amount of energy transfer between the donor and acceptor. Specifically, the donor's lifetime in presence of acceptor (τ_{DA}) is reduced by energy transfer:

$$\tau_D = \tau_o (1-E) \qquad \tau = \tau_o / [1+(R_o/R)^6]$$

As discussed previously, the acceptor has an intrinsic fluorescence lifetime of a few nanoseconds, but because it is continually being excited via energy transfer from the donor, its emission intensity decays with a lifetime that follows the donor's lifetime, τ. The lifetime is

readily tuned by altering the distance (R), and hence energy transfer efficiency, between donor and acceptor.

As proof of principle of these lifetime and color-tailored compounds, here we use oligonucleotide duplexes as a rigid, yet distance-adjustable scaffold, for donor-acceptor pair attachment. The DNA also acts as a means of attaching (hybridizing) the LCTF to target DNA. In principle, the potential exists for making LCTFs for attachment to protein and other targets. Note that this scheme is identical to when one uses LRET to measure distances, but here the donor and acceptor combination is considered as a "black-box" where the interest is in the input parameters (wavelength of excitation) and the output parameters (wavelength, intensity and temporal decay of emission). The distance between donor and acceptor is simply a means to achieve a desired level of energy transfer and is not of interest (or not known) by the user.

We have attached donor-acceptor pairs to DNA in two ways. One method links a lanthanide chelate donor on the 5'-end of a DNA strand, and a fluorescein acceptor in the middle of the *same* strand via C-5 deoxyuridine tethering (Fig. 15). In this method, by choosing an appropriate DNA sequence, the LCTF can bind and label a unique complementary DNA sequence (in a target DNA, for example) with a probe of defined color *and* lifetime —e.g. in fluorescence in-situ hybridization. The other method (Fig. 15) tethers a lanthanide chelate donor on the 5'-end of one DNA strand, and places the acceptor on the 5'-end of a complementary strand, as described previously (55, 77, 78). This attachment mechanism may be useful in chip-based DNA diagnostics and sequencing, because an oligonucleotide can be conveniently synthesized from a solid support with an incorporated acceptor fluorophore, or the support itself may contain an acceptor.

Figure 16 shows the delayed emission spectra of terbium and fluorescein placed on the same strand, separated by either 8 or 10 base pair (Tb-8-FL, Tb-10-FL, respectively), and hybridized to a complementary unlabeled DNA target. Also shown is the terbium-only spectra. The data is collected beginning 30 μsec after pulsed excitation of the sample and consequently, any prompt (nsec) fluorescence of the acceptor has decayed away. The large broad peak around 520 nm is therefore due to fluorescein emission arising only from energy transfer. With greater energy transfer, the Tb-8-FL displays more sensitized emission than the Tb-10-FL. (Tb-6-FL, data not shown, has sufficiently short lifetime that a significant fraction of the signal was lost in the 30 μsec delay time.)

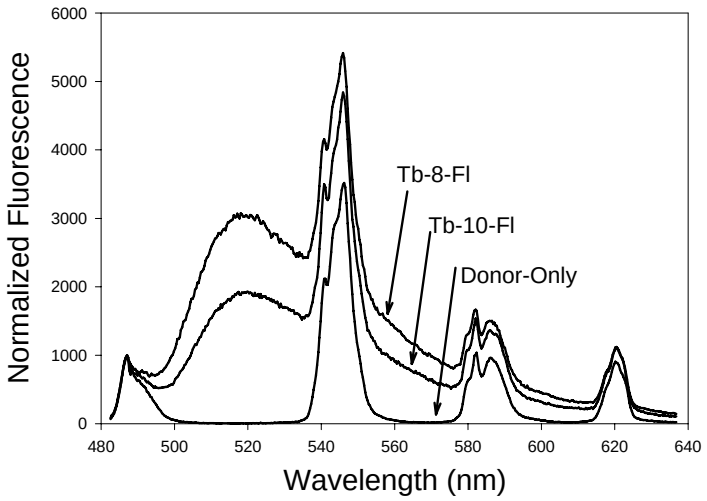

Figure 16. Time-delayed emission spectra of terbium-fluorescein LCTF placed on the same DNA strand, separated by either 8 or 10 base pairs, and hybridized to unlabeled complementary strand. Emission is collected 30 μsec after the excitation pulse; all fluorescein emission (peak at 520 nm) is due to energy transfer from terbium. Energy transfer is larger for the Tb-8-Fl, yielding a larger amount of fluorescein sensitized emission.

Fig. 17 shows the temporal decay of the sensitized fluorescein emission at 518 nm for the Tb-6-FL, Tb-8-FL, Tb-10-FL, and Tb-DNA-donor-only reference. These decays were curve fit to give coefficient-weighted averages of 62, 266, 540, and 1500 μs lifetimes for Tb-6-FL, Tb-8-FL, Tb-10-FL, and Donor-only, respectively. This result clearly shows that the sensitized emission lifetime can be experimentally tuned in the μs time regime. Each LCTF is best fit to a 3-exponential decay, likely caused by the fluorescein acceptor experiencing three different local conformations. Despite this complexity, the average lifetimes are extremely reproducible, with repeat measurements on the same sample within 1% and between different samples within 10%. Hence a target DNA labeled with one of these LCTFs can readily be distinguished from a target DNA labeled with a different LCTFs simply based on lifetimes.

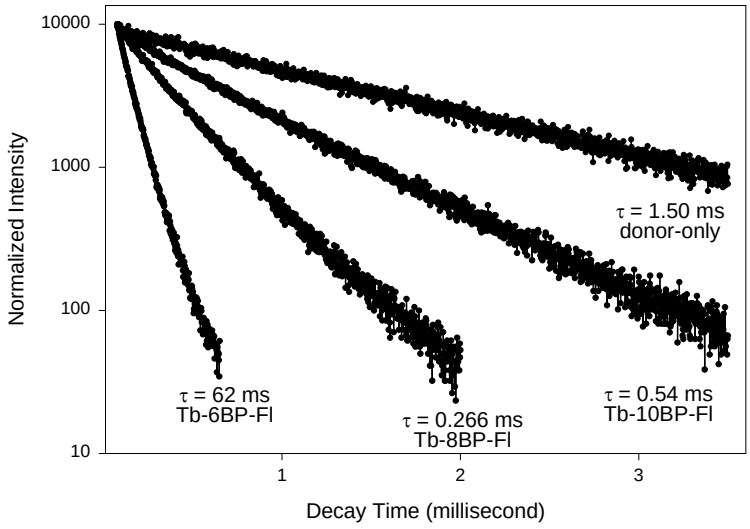

Figure 17. Lifetime decay of fluorescein sensitized emission (520 nm) after receiving energy from terbium donor. The lifetime can be tailored depending on distance between donor and acceptor. Donor and acceptor placed on same strand and hybridized to unlabeled complementary strand.

Fig. 18 shows that different emission colors with similar lifetimes can also be generated by appropriate choice of acceptors, donors, and donor-acceptor distances. Two sets of LCTFs were synthesized. One has Eu^{3+}-chelate as donor on the 5'-end of one strand and Cy5 as the acceptor on the 5'-end of the complementary strand, with 10 base-pairs separating the donor and acceptor. The other has a Tb^{3+}-chelate as donor on the 5'-end of one strand and fluorescein as the acceptor on the 5'-end of the complementary strand, with 8 base pairs separating the donor and acceptor. (The fluorescein was also placed internally on the complementary strand using an abasic fluorescein phosphoramidite with similar results (data not shown).) Fig. 18 shows that the two sensitized emissions have very similar lifetimes, 250 μs for Eu-10-Cy5 pair and 270 μs for Tb-8-Fl pair. However, Cy5 fluoresces around 668 nm (red color) whereas fluorescein emits around 520 nm (green color). These results demonstrate that probes with similar lifetimes, but different emission colors, can be generated.

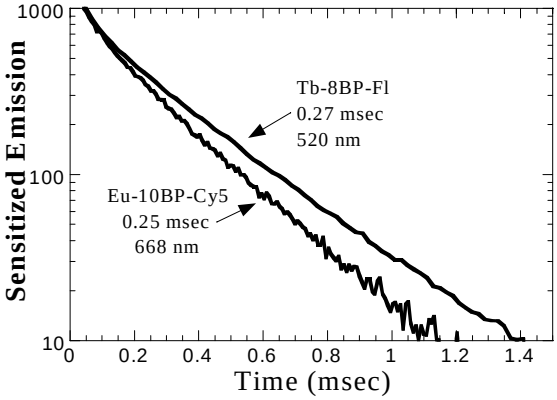

Fig. 18. Similar lifetimes with different emission colors can be generated. The donor was placed on the 5' end of DNA, the acceptor on the 5' end of complementary DNA and the DNAs hybridized. The data is from the sensitized emission lifetime of the acceptor.

Fig. 19 shows the ability to discriminate between a mixture of two probes with the same emission color (detection at 520 nm) but different lifetimes. A Tb-6-Fl DNA ($<\tau>$ = 62 μsec) was mixed with various amounts of Tb-10-Fl ($<\tau>$ = 540 μsec) and the resulting multi-exponential decay was curve-fit to a sum of 6-mer-only and 10-mer-only decays. The population of each species was determined by the relative amplitudes of each component of the fit, and compared to the known amount determined by a simple titration based on absorption measurements at 260 nm. The linearity is quite good (r = 0.993). The slope differs from unity by 24%, but this is within the expected variability due to uncertainty in DNA concentration (approximately +/- 10% for each strand) based on the absorbance titration.

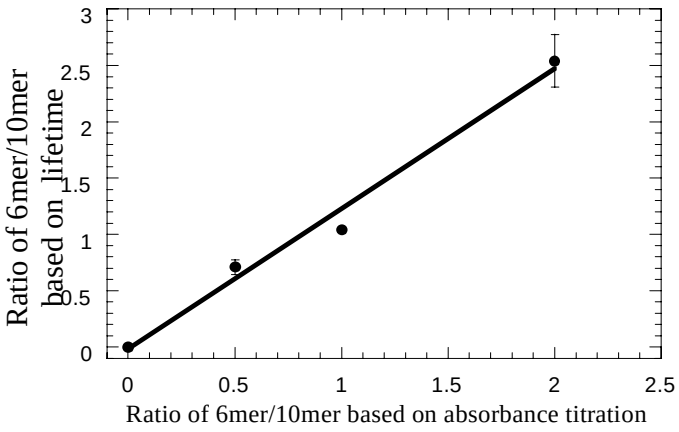

Fig. 19. Two probes with the same emission color (520 nm) but different lifetimes can be independently identified and their populations quantified. Stock solutions of Tb-6-Fl and Tb-10-Fl were mixed at different ratios (determined by absorbance at 260 nm). The sensitized emission lifetime of the mixtures were fit to a sum of the Tb-6-Fl decay and Tb-10-Fl decay and the relative populations determined. The best fit line is: $y = -0.016 + 1.24x$; $r = 0.993$.

The lifetime- and color-tailored dyes reported here open the possibility of quadratically increasing the number of resolvable probes on a single sample, relying not just on conventional color discrimination, but on both color and excited-state lifetime discrimination. If, for example, four colors and four lifetimes can be detected, a target DNA could potentially be labeled with 16 probes, each binding to a unique site, and each probe/sequence uniquely identified by a combination of color and lifetime discrimination. These probes also extend fluorescence lifetime-based detection from the nanosecond range into the tens-to-hundreds of microseconds time domain. This time-scale is long enough to enable facile and nearly complete discrimination against short-lived background fluorescence and scattering, but short enough such that emission rate (saturation) is not a problem in many applications.

Conclusion.

Lanthanides, as alternative probes to conventional fluorophores can lead to enhanced sensitivity in applications where autofluorescence is a problem. Multiple labeling with lanthanide chelates have been shown to be an effective method for further increases in sensitivity. These probes, being nonisotopic, avoid the many practical problems associated with radioactive probes. Lanthanide probes are particularly advantageous in resonance energy transfer, whether to for measuring distances in biocomplexes or used to general new lifetime tailored dyes.

References

1. Alpha, B., Ballardini, R., Balzani, V., Lehn, J.-M., Perathoner, S., Sabbatini, N. (1990) Antenna Effect in Luminescent Lanthanide Cryptates: A Photophysical Study. *Photochem. and Photobiol.* 52: 299-306.
2. Alpha-Bazin, B., Bazin, H., Guillemer, S., Mathis, G. Rare earth cryptates as tool for the study of molecular interactions in biology.
3. Bailey, M. P., Rocks, B. F., Riley, C. (1984) Terbium chelate for use as a label in fluorescent immunoassays. *Analyst* 109: 1449-1450.
4. Benson, S. C., Mathies, R. A., Glazer, A. N. (1993) Heterodimeric DNA-binding dyes designed for energy transfer: stability and applications of the DNA complexes. *Nucl. Acids Res.* 21: 5720-5726.
5. Beverloo, H. B., van Schadewijk, A., Zijlmans, H. J., Verwoerd, N. P., Bonnett, J., Vrolijk, H., Tanke, H. J. (1993) A comparison of the detection sensitivity of lymphocyte membrane antigens using fluorescein and phosphor immunoconjugates. *J Histochem Cytochem* 41: 719-25.
6. Bjartell, A., Laine, S., Pettersson, K., Nilsson, E., Lövgren, T., Lilja, H. (1999) Time-resolved fluorescence in immunocytochemical detection of prostate-specific antigen in prostatic tissue sections. *Histochem J* 31: 45-52.
7. Blomberg, K., Hurskainen, P., Hemmila, I. (1999) Terbium and Rhodamine as Labels in a Homogeneous Time-resolved Fluorometric Energy Transfer Assay of the B Subunit of Human Chorionic Gonadotropin in Serum. *Clinical Chemistry* 45: 855-861.
8. Bunzli, J.-C. G. 1989. *Luminescent Probes*, In Lanthanide Probes in Life, Chemical and Earth Sciences, Theory and Practice, ed. J.-C. G. Bunzli, G. R. Choppin, pp. 219-293. New York: Elsevier
9. Burmeister-Getz, E., Cooke, R., Selvin, P. R. (1998) Luminescence resonance energy transfer measurements in myosin. *Biophys. J.* 75: 2451-2458.
10. Callaci, S., Heyduk, E., Heyduk, T. (1999) Core RNA polymerase from E. coli induces a major change in the domain arrangement of the sigma 70 subunit. *Mol Cell* 3: 229-38.
11. Canfi, A., Bailey, M. P., Rocks, B. F. (1989) Fluorescent Terbium Chelates Derived From Diethylenetriaminepentaacetic Acid and Heterocyclic Compounds. *Analyst* 114: 1405-1406.
12. Canfi, A., Bailey, M. P., Rocks, B. F. (1989) Multiple Labelling of Immunoglobulin G, Albumin and Testosterone With a Fluorescent Terbium Chelate for Fluorescence Immunoassays. *Analyst* 114: 1908-1911.
13. Cantor, C. R., Schimmel, P. R. 1980. *Biophysical Chemistry*. San Francisco: W. H. Freeman and Co.
14. Chen, J., Selvin, P. R. (2000) Lifetime and color-tailored fluorophores in the micro- to milli-second time regime. *J. Am. Chem. Soc.*

15. Chen, J., Selvin, P. R. (in press) Synthesis of 7-Amino-4-trifluoromethyl-2-(1H)-quinolinone and its use as an antenna molecule for luminescent europium polyaminocarboxylate chelates.
16. Chiu, N. H., Christopoulos, T. K., Peltier, J. (1998) Sandwich-type deoxyribonucleic acid hybridization assays based on enzyme amplified time-resolved fluorometry. *Analyst* 123: 1315-9.
17. Christopoulos, T. K., Diamandis, E. P. (1992) Enzymatically Amplified Time-resolved Fluorescence Immunoassay with Terbium Chelates. *Anal. Chem.* 64: 342-6.
18. Clegg, R. M. (1995) Fluorescence Resonance Energy Transfer. *Curr. Op. Biotech.* 6: 103-110.
19. Clegg, R. M. 1996. *Fluorescence Resonance Energy Transfer*, In Fluorescence Imaging Spectroscopy and Microscopy, ed. X. F. Wang, B. Herman, pp. 179-251: John Wiley & Sons, Inc.
20. Coker, G., III, Chen, S. Y., van der Meer, B. W. 1994. *Resonance Energy Transfer*: VCH Publishers, Inc
21. Dahlén, P., Iitiä, A., Mukkala, V. M., Hurskainen, P., Kwiatkowski, M. (1991) The use of europium (Eu^{3+}) labelled primers in PCR amplification of specific target DNA. *Molecular and Cellular Probes* 5: 143-149.
22. Dahlén, P., Liukkonen, L., Kwiatkowski, M., Hurskainen, P., Iitiä, A., Siitari, H., Ylikoski, J., Mukkala, V. M., Lövgren, T. (1994) Europium-Labeled Oligonucleotide Hybridization Probes - Preparation And Properties. *Bioconj. Chem.* 5: 268-272.
23. de Haas, R. R., van Gijlswijk, R. P., van der Tol, E. B., Zijlmans, H. J., Bakker-Schut, T., Bonnet, J., Verwoerd, N. P., Tanke, H. J. (1997) Platinum porphyrins as phosphorescent label for time-resolved microscopy. *J Histochem Cytochem* 45: 1279-92.
24. de Haas, R. R., Verwoerd, N. P., van der Corput, M. P., van Gijlswijk, R. P., Siitari, H., Tanke, H. J. (1996) The use of peroxidase-mediated deposition of biotin-tyramide in combination with time-resolved fluorescence imaging of europium chelate label in immunohistochemistry and in situ hybridization. *J Histochem Cytochem* 44: 1091-9.
25. Diamandis, E., P. (1993) Time-resolved fluorometry in nucleic acid hybridization and Western blotting techniques. *Electrophoresis* 14: 866-875.
26. Diamandis, E., P., Christopoulos, T. K. (1990) Europium Chelate Labels in Time-Resolved Fluorescence Immunoassays and DNA Hybridization Assays. *Anal. Chem.* 62: 1149A-1157A.
27. Dickson, E. F. G., Pollak, A., Diamandis, E. P. (1995) Time-resolved detection of lanthanide luminescence for ultrasensitive bioanalytical assays. *J. Photochem. Photobio B: Biology* 27: 3-19.
28. Dickson, E. F. G., Pollak, A., Diamandis, E. P. (1995) Ultrasensitive Bioanalytical Assays Using Time-Resolved Fluorescence Detection. *Pharmac. Ther.* 66: 207-235.
29. dos Remedios, C. G., Moens, P. D. J. 1998. *Fluorescence resonance energy transfer - applications in protein chemistry*, In Resonance Energy Transfer, ed. D. L. Andrews, A. A. Demidov. Chichester: John Wiley and Sons

30. Evangelista, R. A., Wong, H. E., Templeton, E. F., Granger, T., Allore, B., Pollak, A. (1992) Alkyl- and aryl-substituted salicyl phosphates as detection reagents in enzyme-amplified fluorescence DNA hybridization assays on solid support. *Anal Biochem* 203: 218-26.
31. Fairclough, R., H. , Cantor, C., R. 1978. *The use of Singlet — Singlet Energy Transfer to Study Macromolecular Assemblies*, In Methods in Enzymology, ed. , pp. 347-379
32. Gadella, T. W. J., Jovin, T. M., Clegg, R. M. (1993) Fluorescence Lifetime Imaging Microscopy (FLIM) - Spatial Resolution Of Microstructures On The Nanosecond Time Scale. *Biophysical Chem.* 48: 221-239.
33. Galvan, B., Christopoulos, T. K. (1997) Quantitative reverse transcriptase-polymerase chain reaction for prostate-specific antigen mRNA. 30: 391-7.
34. Galvan, B., Christopoulos, T. K., Diamandis, E. P. (1995) Detection of prostate-specific antigen mRNA by reverse transcription polymerase chain reaction and time-resolved fluorometry. 41: 1705-9.
35. Glazer, A., Mathies, R. (1997) Energy-transfer fluorescent reagents for DNA analyses. *Curr Opin Biotechnol* 8: 94-102.
36. Halonen, P., Rocha, E., Hierholzer, J., Holloway, B., Hyypia, T., Hurskainen, P., Pallansch, M. (1995) Detection of enteroviruses and rhinoviruses in clinical specimens by PCR and liquid-phase hybridization. 33: 648-53.
37. Helmann, J. D., deHaseth, P. L. (1999) Protein-nucleic acid interactions during open complex formation investigated by systematic alteration of the protein and DNA binding partners. *Biochemistry* 38: 5959-5967.
38. Hemmilä, I., Mukkala, V.-M., Takalo, H. J. (1997) Development of luminescent lanthanide chelate labels for diagnostic assays. *J. Alloys Compounds* 249: 158-162.
39. Hennink, E. J., de Haas, R., Verwoerd, N. P., Tanke, H. J. (1996) Evaluation of a time-resolved fluorescence microscope using a phosphorescent Pt-porphine model system. *Cytometry* 24: 312-20.
40. Herman, B. (1989) Resonance Energy Transfer Microscopy. *Meth. Cell Bio.* 30: 219-243.
41. Heyduk, E., Heyduk, T. (1997) Thiol-reactive luminescent Europium chelates: luminescence probes for resonance energy transfer distance measurements in biomolecules. *Anal. Biochem.* 248: 216-227.
42. Heyduk, E., Heyduk, T. (1999) Architecture of a complex between the sigma70 subunit of Escherichia coli RNA polymerase and the nontemplate strand oligonucleotide. Luminescence resonance energy transfer study. *J Biol Chem* 274: 3315-22.
43. Heyduk, E., Heyduk, T., Claus, P., Wisniewski, J. R. (1997) Conformational changes of DNA induced by binding of chironomus high mobility group protein 1a (cHMG1a). *J. Biol. Chem.* 272: 19763-19770.
44. Horrocks, W. D., Jr., Sudnick, D. R. (1979) Lanthanide Ion Probes of Structure in Biology. Laser-Induced Luminescence Decay Constants Provide a Direct Measure of the Number of Metal-Coordinated Water Molecules. *J. Am. Chem. Soc.* 101: 334-350.

45. Iitia, A., Hogdall, E., Dahlen, P., Hurskainen, P., Vuust, J., Siitari, H. (1992) Detection of mutation delta F508 in the cystic fibrosis gene using allele-specific PCR primers and time-resolved fluorometry. 2: 157-62.
46. Ioannou, P. C., Christopoulos, T. K. (1998) Two-round enzymatic amplification combined with time-resolved fluorometry of Tb3+ chelates for enhanced sensitivity in DNA hybridization assays. *Anal Chem* 70: 698-702.
47. Ju, J., Ruan, C., Fuller, C. W., Glazer, A. N., Mathies, R. A. (1995) Fluorescence energy transfer dye-labeled primers for DNA sequencing and analysis. *Proc. Nat. Acad. Sci. USA* 92: 4347-51.
48. Kwiatkowski, M., Samiotaki, M., Lamminmaki, U., Mukkala, V.-M., Landegren, U. (1994) Solid-phase synthesis of chelate-labelled oligonucleotides: application in triple-color ligase-mediated gene analysis. *Nuc. Acids Res.* 22
49. Lakowicz, J. R. 1997. *Long Lifetime Metal-Ligand Complexes as Probes in Biophysics and Clinical Chemistry*, In Methods in Enzymology, ed. L. Brand, M. L. Johnson
50. Lakowicz, J. R. 1999. *Principles of Fluorescence*
51. Lamture, J. B., Wensel, T. G. (1995) Intensely luminescent immunoreactive conjugates of proteins and dipicolinate-based polymeric Tb (III) chelates. *Bioconjug Chem* 6: 88-92.
52. Landegren, U., Kaiser, R., Caskey, C. T., Hood, L. (1988) DNA diagnostics--molecular techniques and automation. *Science* 242: 229-37.
53. Lehn, J. M. 1996. *Comprehensive Supramolecular Chemistry*. New York: PERGAMON/ELSEVIER
54. Li, M., Selvin, P. R. (1995) Luminescent lanthanide polyaminocarboxylate chelates: the effect of chelate structure. *J. Am. Chem. Soc.* 117: 8132-8138.
55. Li, M., Selvin, P. R. (1997) Amine-reactive forms of a luminescent DTPA chelate of terbium and europium: Attachment to DNA and energy transfer measurements. *Bioconjugate Chem.* 8: 127-132.
56. Lövgren, T., Iitia, A. 1995. *Detection of Lanthanide Chelates by Time-Resolved Fluorescence*, In Nonisotopic Probing, Blotting, and Sequencing, ed. , pp. 331-376: Academic Press
57. Malhotra, A., Severinova, E., Darst, S. A. (1996) Crystal structure of a sigma 70 subunit fragment from *E. coli* RNA polymerase. *Cell* 87: 127-36.
58. Mantrova, E. Y., Demcheva, M. V., Savitsky, A. P. (1994) Universal phophorescence immunoassay. *Anal Biochem* 219: 109-14.
59. Marriott, G., Clegg, R. M., Arndt-Jovin, D. J., Jovin, T. M. (1991) Time Resolved Imaging Microscopy. Phosphorescence and Delayed Fluorescence Imaging. *Biophys. J.* 60: 1374-1387.
60. Marriott, G., Heidecker, M., Diamandis, E. P., Yan-Marriott, Y. (1994) Time-resolved delayed luminescence image microscopy using an europium
ion chelate complex. *Biophys. J.* 67: 957-965.

61. Mathis, G. (1993) Rare earth cryptates and homogeneous fluoroimmunoassays with human sera. *Clinical Chem.* 39: 1953-1959.
62. Mathis, G. (1995) Probing molecular interactions with homogeneous techniques based on rare earth cryptates and fluorescence energy transfer. *Clinical Chem.* 41: 1391-1397.
63. Mathis, G., Socquet, F., Viguier, M., Darbouret, B. (1997) Homogeneous immunoassays using rare earth cryptates and time resolved fluorescence: principles and specific advantages for tumor markers. *Anticancer Res* 17: 3011-4.
64. Moronne, M. M. (1999) Development of X-ray excitable luminescent probes for scanning X-ray microscopy. *Ultramicroscopy* 77: 23-36.
65. Periasamy, A., Siadat-Pajouh, M., Wodnicki, P., Wang, X. F., Herman, B. (1995) Time-gated fluorescence microscopy in clinical imaging. *Microscopy and Analysis* 11: 33-35.
66. Prat, O., Lopez, E., Mathis, G. (1991) Europium(III) Cryptate: A Fluorescent label for the Detection of DNA Hybrids on Solid Support. *Anal. Biochem.* 195: 283-289.
67. Ried, T., Baldini, A., Rand, T. C., Ward, D. C. (1992) Simultaneous visualization of seven different DNA probes by *in situ* hybridization using combinatorial fluorescence and digital imaging microscopy. *Proc. Natl. Acad. Sci.* 89: 1388-1392.
68. Root, D. D. (1997) *In situ* molecular association of dystrophin with actin revealed by sensitized emission immuno-resonance energy transfer. *Proc. Natl. Acad. Sci., USA* 94
69. Saha, A. K., Kross, K., Kloszewski, E. D., Upson, D. A., Toner, J. L., Snow, R. A., Black, C. D. V., Desai, V. C. (1993) Time-Resolved Fluorescence of a New Europium Chelate Complex: Demonstration of Highly Sensitive Detection of Protein and DNA Samples. *J. Am. Chem. Soc.* 115: 11032.
70. Samiotaki, M., Kwiatkowski, M., Ylitalo, N., Landegren, U. (1997) Seven-color time-resolved fluorescence hybridization analysis of human papilloma virus types. *Anal Biochem* 253: 156-161.
71. Sammes, P. G., Yahioglu, G. (1996) Modern Bioassays using Metal Chelates as Luminescent Probes. *Natural Products Reports* 13: 1-28.
72. Savitsky, A. P., Chydinov, A. V., Krilova, S. M. 1995. *Novel Fluorescent Chelate for Eu*. Presented at the Advances in Fluorescence Sensing Technology II, San Jose CA 1995
73. Schobel, U., Egelhaaf, H.-J., Brecht, A., Oelkrug, D., Gauglitz, G. (1999) New Donor-Acceptor Pair for Fluorescent Immunoassays by Energy Transfer. *Bioconjugate Chem.* 10: 1107 -1114.
74. Selvin, P. R. 1995. *Fluorescence Resonance Energy Transfer*, In Methods in Enzymology, ed. K. Sauer, pp. 300-334. Orlando: Academic Press
75. Selvin, P. R. (1996) Lanthanide-based resonance energy transfer. *IEEE J. of Selected Topics in Quantum Electronics: Lasers in Biology* 2: 1077-1087.
76. Selvin, P. R. 1999. *Luminescent Lanthanide Chelates for Improved Resonance Energy Transfer and Applications to Biology*, In Applied Fluorescence in Chemistry, Biology and Medicine, ed. W. Rettig, B. Strehmenl, S. Schrader, H. Seifert, pp. 457-487. New York: Springer Verlag

77. Selvin, P. R., Hearst, J. E. (1994) Luminescence energy transfer using a terbium chelate: Improvements on fluorescence energy transfer. *Proc. Natl. Acad. Sci, USA* 91: 10024-10028.
78. Selvin, P. R., Rana, T. M., Hearst, J. E. (1994) Luminescence resonance energy transfer. *J. Am. Chem. Soc.* 116: 6029-6030.
79. Seveus, L., Vaisala, M., Hemmila, I., Kojola, H., Roomans, G. M., Soini, E. (1994) Use of Fluorescent Europium Chelates as Labels in Microscopy Allows Glutaraldehyde Fixation and Permanent Mounting and Leads to Reduced Autofluorescence and Good Long-Term Stability. *Microscopy Res. and Technique* 28: 149-154.
80. Seveus, L., Vaisala, M., Syrjanen, S., Sandberg, M., Kuusisto, A., Harju, R., Salo, J., Hemmilä, I., Kojola, H., Soini, E. (1992) Time-Resolved Fluorescence Imaging of Europium Chelate Label in Immunohistochemistry and *in situ* Hybridization. *Cytometry* 13: 329-338.
81. Sieving, P. F., Watson, A. D., Rocklage, S. M. (1990) Preparation and Characterization of Paramagnetic Polychelates and Their Protein Conjugates. *Bioconj. Chem.* 1: 65-71.
82. Siitari, H., Hemmila, I., Soini, E., Lövgren, T., Koistinen, V. (1983) Detection of hepatitis B surface antigen using time-resolved fluoroimmunoassay. *Nature* 301: 258-60.
83. Sjoroos, M., Iitia, A., Ilonen, J., Reijonen, H., Lovgren, T. (1995) Triple-label hybridization assay for type-1 diabetes-related HLA alleles. *Biotechniques* 18: 870-7.
84. Snyder, G. E., Selvin, P. R. (in prep) Polarization of Luminescent Lanthanide Chelates.
85. Soini, E., Lövgren, T. (1987) Time-Resolved Fluorescence of Lanthanide Probes and Applications in Biotechnology. *CRC Crit. Rev. in Anal. Chem.* 18: 104-154.
86. Speicher, M. R., Gwyn, B. S., Ward, D. C. (1996) Karyotyping human chromosomes by combinatorial multi-fluor FISH. *Nat Genet* 12: 368-75.
87. Stenroos, K., Hurskainen, P., Eriksson, S., Hemmila, I., Blomberg, K., Lindqvist, C. (1998) Homogeneous time-resolved IL-2-IL-2R alpha assay using fluorescence resonance energy transfer. *Cytokine* 10: 495-9.
88. Stryer, L. (1978) Fluorescence Energy Transfer as a Spectroscopic Ruler. *Ann. Rev. Biochem.* 47: 819-846.
89. Takalo, H., Mukkala, V.-M., Mikola, H., Liitti, P., Hemmila, I. (1994) Synthesis of Europium(III) Chelates Suitable for Labeling of Bioactive Molecules. *Bioconjugate Chem.* 5: 278-282.
90. Tanke, H. J., De Haas, R. R., Sagner, G., Ganser, M., van Gijlswijk, R. P. (1998) Use of platinum coproporphyrin and delayed luminescence imaging to extend the number of targets FISH karyotyping. *Cytometry* 33: 453-9.
91. Templeton, E. F., Wong, H. E., Evangelista, R. A., Granger, T., Pollak, A. (1991) Time-resolved fluorescence detection of enzyme-amplified lanthanide luminescence for nucleic acid hybridization assays. *Clin Chem* 37: 1506-12.
92. Vereb, G., Jares-Erijman, E., Selvin, P. R., Jovin, T. M. (1998) Time and spectrally resolved imaging microscopy of lanthanide chelates. *Biophys. J.* **75**: 2210-2222.

93. Verwoerd, N. P., Hennink, E. J., Bonnet, J., Van der Geest, C. R. G., Tanke, H. J. (1994) Use of Ferro-Electric Liquid Crystal Shutters for Time-Resolved Fluorescence Microscopy. *Cytometry* 16: 113-117.
94. Weissman, S. I. (1942) Intramolecular energy transfer: the fluorescence of complexes of europium. *J. Chem. Phys.* 10: 214.
95. Xiao, M., Li, H., Snyder, G. E., Cooke, R., G.Yount, R., Selvin, P. R. (1998) Conformational changes between the active-site and regulatory light chain of myosin as determined by luminescence resonance energy transfer: The effect of nucleotides and actin. *Proc. Nat'l Acad. Sci., USA* 95: 15309-15314.
96. Xiao, M., Selvin, P. R. (1999) An Improved instrument for measuring time-resolved lanthanide emission and resonance energy transfer. *Rev. Sci. Inst.* 70: 3877-3881.
97. Xiao, M., Selvin, P. R. (submitted) Quantum efficiency of luminescent lanthanide chelates and far-red dyes measured by resonance energy transfer. *Proc. Nat'l. Acad. Sci. USA*
98. Xu, J., Root, D. D. (1998) Domain motion between the regulatory light chain and the nucleotide site in skeletal myosin. *J Struct Biol* 123: 150-61.
99. Xu, Y. Y., Pettersson, K., Blomberg, K., Hemmila, I., Mikola, H., Lövgren, T. (1992) Simultaneous quadruple-label fluorometric immunoassay of thyroid- stimulating hormone, 17 alpha-hydroxyprogesterone, immunoreactive trypsin, and creatine kinase MM isoenzyme in dried blood spots. *Clin Chem* 38: 2038-43.
100. Yamada, S., Miyoshi, F., Kano, K., Ogawa, T. (1981) Highly Sensitive Laser Fluorimetry of Europium(III) with 1,1,1-Trifluoro-4-(2-Thienyl)-2,4-Butanedione. *Anal. Chim. Acta* 127: 195-198.
101. Ylikoski, A., Sjoroos, M., Lundwall, A., Karp, M., Lovgren, T., Lilja, H., Iitia, A. (1999) Quantitative reverse transcription-PCR assay with an internal standard for the detection of prostate-specific antigen mRNA. *Clin Chem* 45: 1397-407.